This Accepted Manuscript has not been copyedited and formatted. The final version may differ from this version. A link to any extended data will be provided when the final version is posted online.

eNeuro

Research Article: New Research | Disorders of the Nervous System

An adenosine A_{2A} receptor antagonist improves multiple symptoms of repeated quinpirole induced psychosis

Nozomi Asaoka[1], Naoya Nishitani[1], Haruko Kinoshita[1], Yuma Nagai[1], Hikari Hatakama[1], Kazuki Nagayasu[1], Hisashi Shirakawa[1], Takayuki Nakagawa[2] and Shuji Kaneko[1]

[1]*Department of Molecular Pharmacology, Graduate School of Pharmaceutical Sciences, Kyoto University, 46-29 Yoshida-Shimoadachi-cho, Sakyo-ku, Kyoto, 606-8501, Japan*

[2]*Department of Clinical Pharmacology and Therapeutics, Kyoto University Hospital, 54 Shogoin-Kawahara-cho, Sakyo-ku, Kyoto, 606-8507, Japan*

https://doi.org/10.1523/ENEURO.0366-18.2019

Received: 20 September 2018

Revised: 18 January 2019

Accepted: 26 January 2019

Published: 19 February 2019

N.A., K.N., H.S., T.N., and S.K. designed research; N.A., H.K., and H.H. performed research; N.A., N.N., H.K., Y.N., and H.H. analyzed data; N.A., K.N., and S.K. wrote the paper; N.N. and Y.N. contributed unpublished reagents/analytic tools.

Funding: Japanese Society for the Promotion of Science (JSPS)
16H05091

Funding: http://doi.org/10.13039/100009619Japan Agency for Medical Research and Development (AMED)
18ak0101088h0001

Conflict of Interest: Authors report no conflict of interest.

Japanese Society for the Promotion of Science (JSPS) [16H05091]; Japan Agency for Medical Research and Development (AMED) [18ak0101088h0001]

Correspondence should be addressed to Kazuki Nagayasu, nagayasu@pharm.kyoto-u.ac.jp or Shuji Kaneko, skaneko@pharm.kyoto-u.ac.jp

Cite as: eNeuro 2019; 10.1523/ENEURO.0366-18.2019

Alerts: Sign up at www.eneuro.org/alerts to receive customized email alerts when the fully formatted version of this article is published.

Accepted manuscripts are peer-reviewed but have not been through the copyediting, formatting, or proofreading process.

Copyright © 2019 Asaoka et al.
This is an open-access article distributed under the terms of the Creative Commons Attribution 4.0 International license, which permits unrestricted use, distribution and reproduction in any medium provided that the original work is properly attributed.

eNeuro Accepted Manuscript

eNeuro Accepted Manuscript

Manuscript Title Page

1. Manuscript Title (50 word maximum)

An adenosine A_{2A} receptor antagonist improves multiple symptoms of repeated quinpirole induced psychosis

2. Abbreviated Title (50 character maximum)

Istradefylline rescued quinpirole induced symptoms

3. List all Author Names and Affiliations in order as they would appear in the published article

Nozomi Asaoka[1], Naoya Nishitani[1], Haruko Kinoshita[1], Yuma Nagai[1], Hikari Hatakama[1], Kazuki Nagayasu[1], Hisashi Shirakawa[1], Takayuki Nakagawa[2] & Shuji Kaneko[1]

[1]Department of Molecular Pharmacology, Graduate School of Pharmaceutical Sciences, Kyoto University, 46-29 Yoshida-Shimoadachi-cho, Sakyo-ku, Kyoto 606-8501, Japan

[2]Department of Clinical Pharmacology and Therapeutics, Kyoto University Hospital, 54 Shogoin-Kawahara-cho, Sakyo-ku, Kyoto 606-8507, Japan

4. Author Contributions:

NA, KN, HS, TN, and SK designed the project. NA, HK and HH performed the experiments. NN and YN produced viral vectors. NA, NN, HK, YN and SK analyzed the data. NA, KN, TN, and SK wrote the manuscript. SK supervised the experiments and finalized the manuscript.

5. Correspondence should be addressed to (include email address)

Kazuki Nagayasu

Tel.: +81-75-753-4548; Fax: +81-75-753-4548; E-mail: nagayasu@pharm.kyoto-u.ac.jp

Shuji Kaneko

Tel.: +81-75-753-4541; Fax: +81-75-753-4542; E-mail: skaneko@pharm.kyoto-u.ac.jp

6. Number of Figures: 9 figures

7. Number of Tables: No table

eNeuro Accepted Manuscript

8. Number of Multimedia: 0

9. Number of words for Abstract: 159 words

10. Number of words for Significance Statement: 106 words

11. Number of words for Introduction: 601 words

12. Number of words for Discussion: 1212 words

13. Acknowledgements

This work was supported in part by Grants-in-Aid for Scientific Research (KAKENHI) from the Japanese Society for the Promotion of Science to K.N., H.S., T.N and S.K. and by grant by Japan Agency for Medical Research and Development (AMED) to S.K..

14. Conflict of Interest

Authors report no conflict of interest

15. Funding sources

Japanese Society for the Promotion of Science (JSPS)

16H05091

Japan Agency for Medical Research and Development (AMED)

18ak0101088h0001

eNeuro Accepted Manuscript

Abstract

Obsessive-compulsive disorder (OCD) is a neuropsychiatric disorder characterized by the repeated rise of concerns (obsessions) and repetitive unwanted behavior (compulsions). Although selective serotonin reuptake inhibitors (SSRIs) is the first-choice drug, response rates to SSRI treatment vary between symptom dimensions. In this study, to find a therapeutic target for SSRI-resilient OCD symptoms, we evaluated treatment responses of quinpirole sensitization-induced OCD-related behaviors in mice. SSRI administration rescued the cognitive inflexibility, as well as hyperactivity in the lateral orbitofrontal cortex (lOFC), while no improvement was observed for the repetitive behavior. D_2 receptor signaling in the central striatum (CS) was involved in SSRI-resistant repetitive behavior. An adenosine A_{2A} antagonist, istradefylline, which rescued abnormal excitatory synaptic function in the CS indirect pathway medium spiny neurons of sensitized mice, alleviated both of the QNP-induced abnormal behaviors with only short-term administration. These results provide a new insight into therapeutic strategies for SSRI-resistant OCD symptoms and indicate the potential of A_{2A} antagonists as a rapid-acting anti-OCD drug.

Significance statement

eNeuro Accepted Manuscript

Clinical studies show distinct therapeutic efficacies for SSRIs between subtypes of OCD symptoms. While abnormal activity in the cortico-striatal pathway is critically involved in the pathophysiology of OCD, the neurological mechanisms and therapeutic strategies for SSRI-resistant symptoms remain unclear. In this study, we showed that repeated injection of dopamine D_2 receptor agonist, quinpirole elicited two distinct OCD-related behaviors; cognitive inflexibility (SSRI-responsive) and repetitive behavior (SSRI-resistant). While SSRI treatment normalized hyperactivity of the orbitofrontal cortex, we also demonstrated the imbalanced excitatory inputs in the central striatum of quinpirole-treated mice and the therapeutic potential of an A_{2A} antagonist as a modulator of indirect pathway medium spiny neurons (MSNs).

eNeuro Accepted Manuscript

Introduction

Obsessive-compulsive disorder (OCD) is a psychiatric disorder characterized by repetitive inappropriate thoughts (obsessions) and behaviors to get rid of obsessions (compulsions) (Milad & Rauch, 2012; Bokor & Anderson, 2014). The lifetime prevalence of OCD is approximately 2-3%, and most cases are childhood- or adolescent-onset (Milad & Rauch, 2012; Pauls *et al.*, 2014). Although selective serotonin reuptake inhibitors (SSRIs) are the first-choice treatment for OCD, they require a longer time and higher dose before the onset of therapeutic effects for OCD treatment than for the treatment of major depression (Bokor & Anderson, 2014). Furthermore, even when SSRIs are used properly, 40-60% of patients are resistant to the therapy (Pallanti *et al.*, 2004). Recent evidence has suggested that the efficacies of drug treatment vary by symptom dimensions. For instance, patients with aggression-related obsessions and checking compulsions respond well to SSRI treatment, while sexual/religious obsessions are associated with a poor treatment response (Starcevic & Brakoulias, 2008; Landeros-Weisenberger *et al.*, 2010). In this situation, a novel anti-OCD drug is strongly desired but remains challenging.

OCD was originally classified as an anxiety disorder; however, GABA-enhancing anti-anxiety drugs are ineffective for OCD patients. Whereas anxiety symptoms in OCD patients are heterogeneous, recent clinical studies postulate that cognitive inflexibility

eNeuro Accepted Manuscript

might cause unstoppable obsessions and compulsions, highlighting distinct features of OCD and anxiety disorders (Van Ameringen *et al.*, 2014). Based on these observations, OCD and related disorders have recently been recategorized as a stand-alone group characterized by repetitive behavior in the Diagnostic and Statistical Manual of Mental Disorder (DSM-V; Van Ameringen *et al.*, 2014). Consistent with the updated diagnostic criteria, brain imaging studies have indicated that OCD patients show hyperactivity in cortico-striatal circuits, especially in the orbitofrontal cortex and caudate (Baxter *et al.*, 1987; Graybiel *et al.*, 2000). Hyperactivity of the frontal cortex and striatum was only normalized in patients who responded to SSRI-treatment (Saxena *et al.*, 1999); therefore, control of cortico-striatal pathway activity may be a key for understanding the pathophysiology of OCD and developing novel therapeutic targets for OCD.

Among existing experimental tools for the study of OCD, quinpirole-induced psychosis in rats are known to be an easy-to-use tool (Stuchlik *et al.*, 2016). After several injections of a dopamine D_2 agonist, quinpirole (QNP), rats show several OCD-related behaviors, *e.g.*, robust repetitive checking behavior, which is considered to be similar to the checking compulsion in OCD patients (Szechtman *et al.*, 1998; Stuchlik *et al.*, 2016). However, despite the good similarity in the behavioral phenotype, limited information regarding pharmacotherapeutic response, especially for SSRI

eNeuro Accepted Manuscript

126 treatment, is available (Stuchlik *et al.*, 2016). Considering the limited efficacy of SSRI
127 treatment against several OCD symptoms, an assessment of both SSRI-responsive and
128 SSRI-resistant OCD-like behaviors is beneficial for the elucidation of the
129 pathophysiological and therapeutic mechanisms of OCD.

130 In the present study, we applied the QNP sensitization protocols to mice and
131 characterized OCD-related behavioral and neurological abnormalities. QNP-treated
132 mice showed OCD-like repetitive behavior, cognitive inflexibility, and hyperactivity of
133 the pyramidal neurons in the lateral OFC (lOFC). The cognitive inflexibility and lOFC
134 hyperactivity were rescued by chronic, high-dose SSRI administration, whereas the
135 repetitive behavior was not improved by SSRI administration. SSRI-resistant repetitive
136 behavior was rescued by the local inhibition of D_2 signaling in the central striatum (CS),
137 a projection site of the lOFC. The short-term administration of an adenosine A_{2A}
138 receptor antagonist, istradefylline rescued both of SSRI-responsive and SSRI-resistant
139 OCD-like behaviors in QNP-treated mice. Finally, we showed that electrophysiological
140 studies showed abnormal excitatory inputs to the CS in a cell type-specific manner and
141 these abnormalities were improved by A_{2A} receptor antagonism. The present results
142 offer a new insight into the therapeutic strategy for treatment-resistant OCD.

143

eNeuro Accepted Manuscript

Materials and methods

Reagents

DL-2-Amino-5-phosphonopentanoic acid (DL-APV; an NMDA antagonist; Sigma-Aldrich, St-Louis, MO, USA) and tetrodotoxin (a voltage-dependent Na^+ channel blocker; Sigma-Aldrich) were dissolved in water. (-)-Quinpirole (QNP; a dopamine D_2 agonist; Tocris Bioscience, Bristol, UK) was dissolved in water (for *ex vivo* recordings) or saline (for i.p. injection). 6,7-Dinitroquinoxaline-2,3(1H,4H)-dione (DNQX; an AMPA antagonist; Tocris Bioscience, Bristol, UK), bicuculline (a $GABA_A$ antagonist; Enzo Life Science, Farmingdale, NY, USA), raclopride (a D_2 antagonist; Abcam Biochemicals, Cambridge, UK), PD98059 (a mitogen-activated protein kinase kinase (MEK) inhibitor; Cayman Chemical Company, Ann Arbor, MI, USA) and CGS 21680A (an A_{2A} receptor agonist; Toronto Research Chemicals, Toronto, Canada) were dissolved in dimethyl sulfoxide (DMSO). Stock solutions were stored at -20°C until use and dissolved in saline, artificial cerebrospinal fluid (ACSF) or pipette solution. The final concentration of DMSO was lower than 5% for i.p. injection and microinjection and 0.05% for electrophysiology.

Animals

eNeuro Accepted Manuscript

All animal care and experimental procedures were conducted in accordance with the ethical guidelines of the Kyoto University Animal Research Committee. Male C57BL/6JJmsSlc mice which are the C57BL/6J substrain mice (RRID:IMSR_JAX:000664) maintained at Nihon SLC (Shizuoka, Japan) were purchased and housed at a constant ambient temperature of 24 ± 1°C on a 12-h light-dark cycle with access to food and water *ad libitum*. For behavioral experiments, mice greater than 7 weeks old were used. For the spatial discrimination task, habituation was started at 5 weeks old or older, and training was started at 7 weeks old or older. For electrophysiological recordings, 7-12-week-old mice were used.

For QNP sensitization, mice were intraperitoneally injected with QNP (1 mg/kg) every weekday. For rat, a dose of 0.5 mg/kg was usually used (Szechtman *et al.*, 1998; Servaes *et al.*, 2017). We calculated a dose for mice based on the body surface area (Nair and Jacob, 2016). Mice that received more than 8 injections of QNP were considered QNP-sensitized mice.

For chronic antidepressant treatment, citalopram hydrobromide (FWD Chemicals, Shanghai, China) was dissolved in drinking water (0.2 mg/mL) and administered for 28 days, resulting in an average dose of 24 mg/kg/day (Asaoka *et al.*, 2017). The drug-containing drinking water was shielded from light and changed every 3-5 days.

eNeuro Accepted Manuscript

For the short-term administration of diazepam (0.3 mg/kg), citalopram (10 mg/kg) and istradefylline (3 mg/kg), the drug was intraperitoneally injected 5 min before QNP injection.

Recording of repetitive behavior

Mice were singly or pair-housed, and spontaneous behavior in their home cage was videotaped. Chewing the cage bedding (wood chip) or, in rare cases, the cage mate's hair was considered repetitive (ritual) behavior. Repeated chewing behavior consisted of the following behaviors; holding a wood chip (or fur) in the forelimbs and gently biting and pulling the chip (or hair) by the mouth and forelimbs. At first, we chose the pair-housed condition to reduce stress, but aggressive behavior toward the cage mate was sometimes observed (in both vehicle-treated and drug-treated groups). Therefore, in later experiments, mice were singly housed. There was no apparent difference in repetitive behavior between pair-housed and singly housed mice (Pair-housed mice; 516.8 ± 15.1 s, $n = 16$, Singly housed mice; 532.4 ± 18.38, $n = 19$, $P = 0.5256$ by Student's *t*-test).

Spatial discrimination learning and reversal learning

eNeuro Accepted Manuscript

198 For the spatial discrimination task, mice were food-restricted (2-3 g/day) on weekdays
199 (80-90% of the *ad libitum* body weight; Miyazaki *et al.*, 2014). On the weekend, food
200 was freely available.
201 For the habituation of the mice to the reward (sweetened milk), mice were allowed free
202 access to sweetened milk for approximately 30-60 min. After the 2-day habituation to
203 the reward, mice received pre-training for 4-6 days. In the pre-training period, mice
204 were placed in the T-maze, which consisted of one start arm (30 × 10 cm), two goal
205 arms (30 × 10 cm) and 30-cm-high surrounding walls, and were allowed to freely
206 explore. Both goal arms were rewarded during the pre-training period.
207 Spatial discrimination tests were performed as previously described (Moy *et al.*, 2007,
208 Bannerman *et al.*, 2008) with several modifications. Mice received 6 or 7-day training
209 and 8-day overtraining (Smith *et al.*, 2012). During these periods, mice were trained for
210 5 free-choice trials per day. The rewarded goal arm (rewarded with 100 μL of sweetened
211 milk) was randomly chosen and fixed during the training and overtraining periods. At
212 the entrance of each goal arm, a guillotine door was placed, and once the mice entered
213 the goal arm, the door was immediately closed. Mice were returned to their home cage
214 during the preparation for the next trial (approximately 2 min).
215 On the 7^{th} or 8^{th} training day, the correct choice rate during the previous three days was

eNeuro Accepted Manuscript

calculated, and mice that showed a correct choice rate of greater than 75% were used for the subsequent overtraining. The day that the mice met this criterion was considered to be Day 1 of the overtraining period (OT1).

During the overtraining period, mice received similar spatial discrimination training as in the previous training period combined with QNP injection (1 mg/kg, i.p.). The effects of reduced locomotion by an acute QNP injection were avoided by injecting QNP after training on the first 2-3 overtraining days (OT1-2 or 3) and then 20-30 min after training on OT3 or 4-8. For the second criterion, the correct choice rate during OT4-OT8 was calculated, and mice that showed a correct choice rate of more than 80% were used for the reversal learning test.

For reversal learning, the rewarded arm was reversed, and mice underwent 10 free-choice trials per day for 4 days (R1-4). During this period, QNP was injected 20-30 min before starting experiments.

The spatial discrimination task without an overtraining period (Figure 2h) consisted of an 8-day training period (T1-8) and a 4-day reversal learning period (R1-4). QNP was injected after (T1-2) and before (T3-8, R1-4) experiments.

Elevated plus maze test

eNeuro Accepted Manuscript

234 The elevated plus maze consisted of two open arms and two closed arms (30 × 5 cm)
235 extended from a central platform (5 × 5 cm). After 25 min of drug injection, mice were
236 placed on the central platform and monitored for 5 min. The time spent in each arm was
237 analyzed using a video tracking system (ANY-maze version 4.99).
238
239 **Open field test**
240 After 25 min of drug injection, mice were placed at the center of an open field (75 ×
241 75 cm; without a wall; Szechtman *et al.*, 1994) and monitored for 10 min. The total
242 distance traveled was analyzed using a video tracking system (ANY-maze version 4.99).
243
244 **Preparation of the adeno-associated virus (AAV) vector**
245 Lenti-X 293T cells were transfected with pAAV-hSyn1-Venus, pAAV-DJ, and pHelper
246 using polyethylenimine (polyethylenimine “Max", Polysciences), and 72 h after
247 transfection, the cells were gently scraped with a gradient buffer (composition in mM; 1
248 Tris, 15 NaCl and 1 $MgCl_2$). The buffer was freeze-thawed four times between liquid
249 nitrogen and a 55°C water bath to break the cell membrane. DNA and RNA were
250 removed by benzonase nuclease (Sigma), and cell debris was removed by centrifugation
251 at 3,000 g for 15 min. Viral stocks were purified using four different layers of an

eNeuro Accepted Manuscript

252 iodixanol (Opti Prep, Sigma) gradient, *i.e.,* 15%. 25%, 40%, and 58%. After
253 ultracentrifugation for 105 min at 48000 rpm, the viral fraction was extracted from the
254 interface between the 40% and 58% layers.
255
256 **Stereotaxic surgery and microinjection**
257 Mice were anesthetized with sodium pentobarbital (50 mg/kg, i.p., Nakarai Tesque,
258 Kyoto, Japan) and fixed on a small animal stereotaxic frame (Narishige, Tokyo, Japan).
259 For lOFC neuronal labeling, 0.75 μL AAV-hSyn1-Venus was microinjected into the
260 lOFC (AP +2.7 mm, ML +1.7 mm, DV +2.7 mm from bregma). After 4 weeks, mice
261 were decapitated, and coronal forebrain slices were prepared by using a vibratome (see
262 "Preparation of acute brain slices for electrophysiological analysis"). Forebrain slices
263 were fixed in 4% paraformaldehyde. After fixation, slices were washed in
264 phosphate-buffered saline, and the green fluorescence of Venus was visualized using a
265 Nikon Diaphot 200 microscope equipped with a laser scanning confocal imaging system
266 (MRC-1024, Bio-Rad Laboratories, Hercules, CA).
267 For drug microinjection, mice were implanted with a bilateral guide cannula directed
268 at the central striatum (CS; AP +1.2 mm, ML +2.0 mm, DV +3.8 mm from bregma,
269 angled 10°) and fixed to the skull by dental cement. On the experimental day, the

eNeuro Accepted Manuscript

injection cannula was inserted into the guide, and drug (1 μg raclopride or PD98059 in 1 μL or 0.3 ng CGS 21680A in 1 μL) was injected at a rate of 0.15 μL/min. After injection, the injection cannula was left in place for for 5 min (for raclopride) or 10 min (for PD98059). For CGS 21680A, the injection cannula was left during the recording. After experiments, 0.5 μL of Evans Blue solution was injected through the cannula to confirm the injection site. When injection site was incorrect, the animal was excluded from analysis.

Preparation of acute brain slices for electrophysiological analysis

For electrophysiological analysis, mice were received 8 injections of QNP or saline and the next day after the 8th injection, acute brain slices were prepared. Mice were deeply anesthetized with isoflurane and decapitated. The brains were rapidly collected in ice-cold cutting solution (composition in mM: 120 N-Methyl-D-glucamin-Cl, 2.5 KCl, 26 $NaHCO_3$, 1.25 NaH_2PO_4, 0.5 $CaCl_2$, 7 $MgCl_2$, 15 D-glucose, and 1.3 ascorbic acid, pH 7.2). Coronal brain slices (200-μm thick) were prepared with a vibratome (VT1000S, Leica, Wetzlar, Germany). For recording from the CS, slices were dissected from relatively anterior part of the striatum, where OFC send dense projections (Hunnicutt et al., 2016). Slices were recovered in oxygenated ACSF (composition in

eNeuro Accepted Manuscript

288 mM: 124 NaCl, 3 KCl, 26 $NaHCO_3$, 1 NaH_2PO_4, 2.4 $CaCl_2$, 1.2 $MgCl_2$, and 10
289 D-glucose, pH 7.3) at 32°C for at least 1 h before recording. After recovery, individual
290 slices were transferred to a recording chamber with continuous perfusion of oxygenated
291 ACSF at a flow rate of 1–2 mL/min. ACSF was warmed to keep the recording chamber
292 at 27 ± 1°C. Recordings were performed only within 4 h after recovery.
293
294 **Electrophysiological recordings**
295 Electrophysiological recordings were performed with an EPC9 amplifier (HEKA,
296 Pfalz, Germany), and the data were recorded using Patchmaster software (HEKA). The
297 resistance of the electrodes was 3-6 MΩ when filled with the internal solution
298 (composition in mM: 140 K-gluconate, 5 KCl, 10 HEPES, 2 Na-ATP, 2 $MgCl_2$, and 0.2
299 EGTA, pH 7.3 adjusted with KOH for current-clamp recordings and EPSC recordings
300 from the lOFC; 70 K-gluconate, 75 KCl, 10 HEPES, 2 Na-ATP, 2 $MgCl_2$, and 0.2
301 EGTA, pH 7.3 adjusted with KOH for IPSC recordings; and 120 $CsMeSO_4$, 15 CsCl, 8
302 NaCl, 10 HEPES, 2 Mg-ATP, 0.3 Na-GTP, 0.2 EGTA, 10 TEA-Cl, and 5 QX-314, pH
303 7.3 adjusted with CsOH for EPSC recordings from the striatum). Individual neurons
304 were visualized with a microscope equipped with a 40 × water-immersion objective lens
305 (Carl Zeiss, Jena, Germany) and a CCD camera. The series resistance was compensated

eNeuro Accepted Manuscript

306 by 70% and maintained within 35 MΩ.

307 For recording from lOFC pyramidal neurons, a current injection (100-300 pA, 1-s
308 duration) was performed to elicit action potentials. As previously reported (Tateno &
309 Robinson, 2006), pyramidal neurons showed regular-spiking activity (Figure 1A and D),
310 whereas interneurons showed fast-spiking activity (Figures 1B-D). lOFC neurons
311 showing regular-spiking activity were used for experiments. Action potentials were
312 evoked by current injection (0-500 pA, 1-s duration). EPSCs were recorded with bath
313 application of the $GABA_A$ antagonist (20 μM bicuculline), while AMPA/NMDA
314 antagonists (20 μM DNQX and 50 μM APV) were applied to record IPSCs.
315 Tetrodotoxin (0.3 μM) was added to the bath solution for recording miniature EPSCs
316 and IPSCs. Events were analyzed by Minianalysis software (SynaptoSoft, Decatur, GA).
317 The membrane potential during voltage-clamp recordings was held at -70 mV.

318 For the recordings from CS MSNs, MSNs were determined by their morphological
319 features, and after the recording, single-cell PCR was performed to identify the cell type.
320 For acute QNP treatment, QNP (10 μM) was bath applied for at least 3 min. For
321 electrical stimulation, a stimulation electrode was placed near the recording electrode.
322 AMPA-mediated eEPSCs and mixed AMPA and NMDA-mediated eEPSCs were
323 evoked by stimulation at -70 mV and +40 mV, respectively. NMDA-mediated eEPSC

eNeuro Accepted Manuscript

amplitude was determined as the average amplitude between 45 and 55 ms after stimulation. The average of 3 NMDA/AMPA ratio measurements was used for analysis.

Single-cell reverse transcription-polymerase chain reaction (RT-PCR)

After the whole-cell recording, the contents of the cell were aspirated into the recording pipette and harvested in a sampling tube. The collected samples were reverse-transcribed using a ReverTra Ace RT kit (TOYOBO, Tokyo, Japan) and amplified with Blend Taq (TOYOBO, Tokyo, Japan). The oligonucleotide primers used were 5'- CCCAGGCGACATCAATTT-3' and 5'-TCTCCCAGATTTTGAAAGAAGG-3' for proenkephalin (*Penk*); 5'-CCAGGGACAAAGCAGTAAGC-3' and 5'- CGCCATTCTGACTCACTTGTT-3' for prodynorphin (*Pdyn*); and 5'-CCGCTGATCCTTCCCGATAC-3' and 5'-CGACGTTGGCTGTGAACTTG-3' for enolase 2 (*Eno2*) as a neuronal marker. The PCR products were analyzed using agarose gel electrophoresis. *Pdyn*-positive neurons were considered to be direct pathway MSNs (dMSNs), and *Pdyn*-negative and *Penk*-positive neurons were considered to be indirect pathway MSNs (iMSNs) (Figures 2A and B).

eNeuro Accepted Manuscript

342 **Experimental design and Statistical analysis**

343 All data are presented as the mean ± standard error of mean (S.E.M). Statistical
344 analysis was performed with GraphPad Prism 5 (GraphPad, San Diego, CA, USA;
345 RRID:SCR_002798). Differences with $P < 0.05$ were considered significant. The
346 differences between two groups were compared by a two-tailed Student's *t* test or
347 unpaired *t* test with Welch's correction. When differences within a mouse were
348 compared, a two-tailed paired *t*-test was used for analysis. The differences between
349 more than three groups were compared by one-way analysis of variance (ANOVA) with
350 *post hoc* Tukey's multiple comparison test. For examination of the time-course or
351 current injection experiments, two-way ANOVA for repeated measures and following
352 Bonferroni post-test was used for analysis. Before performing repeated measures
353 ANOVA, Mauchly's sphericity test were performed by using R (version 3. 5. 2;
354 RRID:SCR_001905) and when the assumption of sphericity is violated, the
355 Greenhouse-Geisser correction was used. Changes in the NMDA/AMPA ratio were
356 analyzed by one-sample t-test.

357

358 **Results**

359 ***Repeated injection of quinpirole induced OCD-related behaviors and lOFC***

eNeuro Accepted Manuscript

hyperactivity

First, we produced QNP-sensitized mice and characterized their behavioral and neurological changes. Mice received a QNP (1 mg/kg) injection every weekday, and after 8-9 injections, QNP-treated mice showed more locomotor activity in the open field than saline-treated mice (Figures 3A and D) but did not display any anxiogenic effects in the elevated-plus maze test (Figures 3A-C). Hyper-locomotion in the open field is reported to be a feature of QNP sensitization in rats (Szechtman *et al.*, 1994), and thus, this result was indicative of the successful establishment of QNP sensitization in mice.

Repetitive behaviors are one of the widely accepted OCD-related behaviors in rodents (Boulougouris *et al.*, 2009, Camilla d'Angelo *et al.*, 2014; Zike *et al.*, 2017). Following 3 to 4 injections of QNP, mice showed repeated chewing behavior in their home cages (chewing wood chip bedding or cage mate's hair; see "Recording of repetitive behavior" in Materials and Methods). This repetitive behavior peaked after 8 injections (Figures 3E and F,). Additional injection of QNP (total 9-12 injections) did not induce further changes in the duration of chewing behavior (Figure 3I, "QNP+Saline group"). This robust chewing was only observed after the QNP injection and was eliminated within 60 min of the injection (Figure 3G). Therefore, the repeated injection and challenge with QNP induced repetitive behavior. In addition, the short-term administration of diazepam

eNeuro Accepted Manuscript

(0.3 mg/kg) and citalopram (10 mg/kg), which do not show therapeutic effects in OCD patients, had no effect on the chewing behavior (Figures 3H and I).

Recent clinical evidence has suggested that OCD patients exhibit cognitive inflexibility and increased reliance on habitual responses (Gillan *et al.*, 2011; Gillan *et al.*, 2016). To assess this feature, we performed a spatial discrimination and reversal learning task. Daily QNP injection did not affect spatial learning (Figures 3J and K), indicating that the repeated QNP injection did not affect goal-directed learning. In a spatial discrimination task, longer training period enhances habitual learning (Smith *et al.*, 2012). To assess whether QNP-treated mice showed cognitive inflexibility after longer learning period, mice received modest overtraining (5 trials/day, 8 days) after the training period (Figures 3L and M). Under this condition, saline-treated mice still showed flexible behavior, while QNP-treated mice displayed a deficit in reversal learning (Figure 3N), indicating that QNP-treated mice easily exhibit habit-like inflexible behavior.

Clinical studies have suggested that activity in the lateral OFC (lOFC) is higher in OCD patients than in healthy controls and that successful SSRI treatment normalizes this activity (Baxter *et al.,* 1987; Saxena *et al.,* 1999). To determine whether QNP-treated mice show OCD-like neurological abnormalities, the firing activity was

eNeuro Accepted Manuscript

recorded by using *ex vivo* electrophysiological recording from lOFC pyramidal neurons (Figure 4A). lOFC pyramidal neurons from QNP-treated mice showed a higher firing response than those from saline-treated mice. This increase was abolished in the presence of AMPA and NMDA antagonists (20 μM DNQX and 50 μM AP-V) (Figures 4B and C). There was no difference between the resting membrane potential of pyramidal neurons from QNP and saline-treated mice (Saline group; -80.41 ± 1.23 mV, n = 10 from 3 mice, QNP group; -81.25± 2.02 mV, n = 11 from 3 mice, P = 0.7358 by Student's t-test). Both the spontaneous and miniature EPSC frequencies in lOFC pyramidal neurons were significantly higher in QNP-treated mice than in saline-treated mice (Figures 4D, E and G), while no change in the EPSC amplitude was observed (Figures 4F and H), suggesting a plastic change in the glutamatergic synapses in the lOFC of QNP-treated mice.

Chronic SSRI administration rescued the cognitive inflexibility and neurological deficits but not the repetitive behavior in QNP-treated mice

To examine the treatment response to a high dose of an SSRI, mice were treated with citalopram (24 mg/kg/day) for 28 days. In QNP-treated mice, although the SSRI failed to reduce the repetitive chewing behavior (Figures 5A and B), SSRI treatment improved

eNeuro Accepted Manuscript

414 the reversal learning in the spatial discrimination task combined with overtraining
415 (Figures 5C-E).

416 In electrophysiological recordings, SSRI treatment decreased the firing activity of
417 lOFC pyramidal neurons in QNP-treated mice (Figures 6A and B). The inhibitory effect
418 of SSRI treatment was suppressed by a $GABA_A$ antagonist (Figure 6C). No differences
419 were observed in the spontaneous IPSC amplitude or in the miniature IPSC frequency
420 and amplitude between SSRI-treated and treatment-free QNP-treated mice (Figures 6D,
421 F-H), whereas the spontaneous IPSC frequency was increased in the SSRI plus
422 QNP-treated mice compared to that in the QNP-only treated mice (Figure 6E),
423 suggesting that SSRI treatment increased the GABAergic inhibition of lOFC pyramidal
424 neurons.

425

426 ***D_2-ERK signaling in the CS is involved in SSRI-resistant repetitive behavior in***
427 ***QNP-treated mice***

428 Although lOFC hyperactivity was improved by chronic SSRI treatment, the repetitive
429 chewing behavior was not reversed. Since the OFC-striatum pathway is activated in
430 OCD patients (Baxter *et al.*, 1987; Beucke *et al.*, 2013), we hypothesized that synaptic
431 changes in the lOFC-striatum pathway might be involved in the chewing behavior in

eNeuro Accepted Manuscript

QNP-treated mice. To test this hypothesis, we first confirmed the projection site of lOFC neurons in the striatum. For lOFC neuronal labeling, an adeno-associated virus that expressed Venus protein (AAV-hSyn-Venus) was injected into the lOFC (Figure 7A). Consistent with a previous report (Gremel *et al.*, 2016), green fluorescence-positive terminals were observed in the central part of the striatum (CS), which is functionally classifies as a part of the associative striatum (Chuhma *et al.*, 2016), indicating the presence of lOFC inputs in the CS (Figure 7B).

Robust chewing behavior was observed only after challenge with QNP, suggesting that not only chronic changes but also the stimulation of D_2 receptors were necessary for the induction of chewing behavior. To identify the contribution of D_2 receptors in the CS, we performed a local bilateral injection of a D_2 antagonist, raclopride (1 μg/side), in the CS (Figure7C). After the raclopride injection, QNP failed to elicit repetitive chewing in QNP-treated mice (Figure 7D), indicating that D_2 receptor signaling in the CS is required for repetitive chewing in QNP-treated mice.

In striatal neurons, the stimulation of D_2 receptors activates extracellular signal-regulated kinase (ERK) (Brami-Cherrier *et al.*, 2002, Shioda *et al.*, 2017). The local bilateral injection of a MEK/ERK inhibitor, PD98059 (1 μg/side), in the CS significantly reduced QNP-induced chewing behavior (Figure 7E), suggesting the

eNeuro Accepted Manuscript

involvement of D_2 receptor signaling-induced activation of the MEK/ERK pathway in repetitive chewing.

Adenosine A_{2A} receptors are G_s-coupled receptors that modulate ERK activation (Moreau *et al.*, 1999). Because, in the striatum, A_{2A} receptors are expressed in iMSNs but not dMSNs (Calabresi *et al.*, 2014), we hypothesized that stimulation of A_{2A} receptors facilitates D_2 receptor stimulation-induced chewing behavior in QNP sensitized mice. To test this hypothesis, we examined the effects of intra-CS injection of an A_{2A} receptor agonist on subthreshold dose of QNP-induced behavior. For the definition of the subthreshold dose of QNP, we examined three different doses of QNP (1.0, 0.5, 0.3 mg/kg, i.p.). After 7-time injection of normal dose of QNP (1 mg/kg), mice were received different dose of QNP challenge (Figure 7F). At the dose of 0.5 mg/kg, there seemed a slight decrease in chewing behavior, whereas chewing behavior was not observed at 0.3 mg/kg (Figure 7G). From these results, we defined a dose of 0.3 mg/kg as subthreshold dose of QNP. Next, we examined the effects of a combination of an A_{2A} receptor agonist (CGS 21680A; CGS) and subthreshold dose of QNP. After sensitization, CGS (0.3 ng/side) or vehicle was infused into the CS and concurrently, subthreshold dose of QNP (0.3 mg/kg, i.p.) was injected (Figure 7H). CGS + QNP elicit significant increase in chewing behavior compared to Veh + QNP (Figure 7I), even though CGS +

eNeuro Accepted Manuscript

468 QNP-induced chewing duration was short relative to that induced by the normal dose of
469 QNP. The leading causes of this weak effect may be sedative effect of the combination
470 treatment. While CGS alone and subthreshold dose of QNP did not cause sedation, CGS
471 + QNP showed sedative effects, suggesting that CGS + QNP combination facilitated
472 both QNP-induced chewing behavior and CGS-induced sedative effect (Barraco *et al*.,
473 1994; Chen *et al*., 2001). Despite the lowered locomotion, CGS + QNP showed
474 significant increase in chewing behavior and, indicating the involvement of A_{2A} receptor
475 signaling in the CS on QNP-induced repetitive chewing behavior.
476
477 ***Istradefylline rescued both the behavioral and cognitive symptoms in QNP-treated***
478 ***mice***
479 The local injection experiments indicate the involvement of A_{2A} receptor and
480 MEK/ERK signaling on QNP-induced behavioral abnormality, we assumed that an A_{2A}
481 receptor antagonist could rescue QNP-induced chewing behaviors. A single
482 administration of an A_{2A} receptor antagonist, istradefylline (3 mg/kg), significantly
483 decreased the total chewing time in QNP-treated mice, and this effect was potentiated
484 following repeated injections (Figures 8A and B). In addition to the effect on the
485 repetitive behavior, the short-term administration of istradefylline improved reversal

eNeuro Accepted Manuscript

learning in QNP-treated mice (Figures 8C-E), suggesting the rapid effects of istradefylline on both SSRI-responsive and SSRI-resistant symptoms.

Istradefylline rescued the altered synaptic plasticity in CS iMSNs from QNP-treated mice

Rapid effects of istradefylline on SSRI-resilient chewing behaviors suggests a different action mechanism of istradefylline from that of chronic SSRI. Therefore, we tested the above-mentioned hypothesis that istradefylline acts on the CS iMSNs by using electrophysiological recordings (Figure 9A).

First, to investigate repeated QNP injection-induced changes in the CS MSNs, we recorded the basal NMDA/AMPA ratios of the CS MSNs from mice received repeated QNP or saline injection.. Compared to the saline-treated mice, the basal NMDA/AMPA ratio was increased in iMSNs from QNP-treated mice, whereas no significant changes were observed in dMSNs (Figures 9B and C). In addition, to examine the effects of challenge with QNP, we compared NMDA/AMPA ratios before (basal) and after the bath application of QNP (10 μM), which mimics an *in vivo* challenge with QNP. In contrast to the basal NMDA/AMPA ratio, the bath application of QNP (10 μM) induced a significant reduction in the NMDA/AMPA ratio in iMSNs from QNP-treated mice but

eNeuro Accepted Manuscript

not from saline-treated mice (Figures 9D and E). The intracellular application of PD98059 (50 μM) through the recording electrode restored those abnormal synaptic functions for both baseline and QNP application induced-responses (Figures 9C and E), suggesting that, in QNP-treated mice, CS iMSNs showed altered synaptic plasticity through D_2-ERK signaling.

We then examined the effects of istradefylline on the QNP-induced synaptic changes. As expected, the bath application of istradefylline (10 μM) had no effects on the NMDA/AMPA ratios recorded from the CS dMSNs (Figures 9B and C). In case of iMSNs, bath application of istradefylline tend to increase the baseline NMDA/AMPA ratio from saline-treated mice and no further increase was observed in QNP-treated mice (Figure 9D). The QNP application induced-response in iMSNs from QNP-treated mice was also inhibited by bath application of istradefylline (Figure 9E).

Discussion

In this study, we characterized QNP sensitization-induced OCD-related behaviors and treatment responses in mice. Both the cognitive inflexibility and the abnormal lOFC activity in QNP-treated mice were rescued by chronic high-dose SSRI, whereas these treatments failed to improve the repetitive chewing behavior. Finally, we showed that D_2

eNeuro Accepted Manuscript

522 signaling in CS iMSNs, where lOFC neurons project, was required for this repetitive
523 behavior and that the short-term administration of a clinically approved A_{2A} antagonist,
524 istradefylline, rescued both SSRI-responsive and SSRI-resistant symptoms in
525 QNP-treated mice.
526
527 As OCD-like behaviors in rodents, most existing reports evaluate repetitive behaviors
528 (*e.g.*, excessive grooming) and perseverative behaviors (*e.g.*, deficits in spontaneous
529 alternation and reversal learning) (Alonso *et al.*, 2015; Stuchlik *et al.*, 2016). However,
530 the pathophysiological mechanisms of those OCD-like behaviors are not fully
531 understood, especially about the differences in the neurological and therapeutic
532 mechanisms between the two symptoms (Alonso *et al.*, 2015; Stuchlik *et al.*, 2016).
533 QNP-treated mice exhibited both of these behaviors, demonstrating that the
534 QNP-induced behavioral abnormalities in mice are convenient for examining
535 pathophysiological mechanisms and subsequent drug screening.
536 Dopaminergic drug-induced repetitive behaviors are widely reported both in basic and
537 clinical studies. In animal experiments, single administration of psychostimulant elicits
538 various stereotypic behaviors, including chewing and grooming (Izawa *et al.*, 2006;
539 Milesi-Hallé *et al.*, 2007). Recent evidence demonstrated the modulating effects of

eNeuro Accepted Manuscript

mutation of OCD-related gene in psychostimulant-induced stereotypy (Zike *et al.*, 2017). In psychostimulant abusers and parkinsonian patient with dopaminergic replacement therapy, non-goal-directed complex stereotypies, which are similar to OCD symptoms, are observed (Voon *et al.*, 2009; Fasano *et al.*, 2010). These observations suggest the existence of the common mechanisms underlying OCD and dopaminergic drug-induced stereotypies. Based on this, QNP-induced repetitive chewing might also share the common mechanisms, while further discrimination against other repetitive behaviors, such as tic disorder which is often comorbid with OCD, should be carefully performed.

SSRIs are the first-choice drugs for OCD patients, and in SSRI-responsive patients, SSRIs normalizes the activity of the anterior lOFC (Saxena *et al.*, 1999). The OFC can be divided into the medial OFC (mOFC) and the lOFC, which encode essentially similar but distinct information (Milad & Rauch, 2012). For instance, the mOFC is activated by positive reward stimuli, while the lOFC responds to punishment (Ursu & Carter, 2005; Plassmann *et al.*, 2008). OCD patients exhibit a deficiency in punishment-related learning (Nielen *et al.*, 2009), and possibly as a result of this abnormal punishment processing, OCD patients, especially in severe cases, are unable to stop their compulsions, even when the compulsions cause a disadvantage to the

eNeuro Accepted Manuscript

patients themselves (Pauls *et al.*, 2014). In this situation, lOFC hyperactivity might be one of the common neurological bases and a therapeutic target for cognitive inflexibility among OCD patients and QNP-treated mice.

In contrast to cognitive inflexibility, repetitive chewing behavior was SSRI-resistant, suggesting that the inhibition of lOFC outputs was insufficient to improve repetitive behavior. Recent optogenetic research demonstrated that the repeated activation of the OFC-striatum pathway increased grooming behavior (Ahmari *et al.*, 2013), and the overall inhibition of the OFC-striatum pathway contributed to the inhibition of compulsive grooming behavior in a genetic OCD model, the *Dlgap3* (*Sapap3*)-knockout mice (Burguière *et al.*, 2013). However, both in the optogenetic stimulation model and *Sapap3*-knockout mice, repetitive behavior was reduced by SSRI administration (Welch *et al.*, 2007, Burguière *et al.*, 2013). One possible reason for this discrepancy is that the input-output balance between striatal dMSNs and iMSNs was differentially altered in QNP-treated mice and the overall decrease in lOFC inputs failed to rectify the abnormal activity balance between MSN subtypes. In other word, after challenge with QNP, the OFC-striatum iMSN pathway rather than the OFC-striatum dMSN pathway was potentiated, causing the abnormal transmission of OFC information. While further experiments on the pathway-specific control are required, hyperactivity in the lOFC-CS

eNeuro Accepted Manuscript

iMSN pathway might contribute to SSRI-resistant repetitive behavior in QNP-treated mice.

Changes in the activity balance between iMSNs and dMSNs contributes to habit formation (Shan *et al.*, 2015; O'Hare *et al.*, 2016). Recent research demonstrated that the selective reduction of excitatory inputs from the OFC to striatal dMSNs promotes habit formation (Renteria *et al.*, 2018). Considering that habit learning is facilitated in OCD patients (Gillan *et al.*, 2011; Gillan *et al.*, 2016), this finding supports the idea that an abnormal activity balance between iMSNs and dMSNs contributes to OCD pathophysiology. Considering that the OFC-striatum pathway contributes to goal-directed behavior, and the activation of the OFC promotes a goal-directed behavioral pattern rather than habit formation (Gremel & Costa, 2013; Gourley & Taylor, 2016), an abnormal activity balance between iMSNs and dMSNs might explain the clinical features of OCD.

Although the D_2 receptor signal theoretically inhibits neurons, a recent study demonstrated that the acute activation of D_2 receptors does not inhibit iMSNs (Lemos *et al.*, 2016), possibly because of the lack or low levels of expression of G protein-coupled inwardly rectifying potassium channels in iMSNs (Kobayashi *et al.*, 1995). The sustained activation of D_2 receptors by a selective agonist activates ERK signaling in

eNeuro Accepted Manuscript

iMSNs, possibly through D_2 receptor internalization (Brami-Cherrier *et al.*, 2002; Shioda *et al.*, 2017), resulting in the activation of rather than the inhibition of iMSNs. Supporting this idea, both in OCD patients and in QNP-sensitized rats after challenge with QNP, D_2 receptor occupancy was decreased (Denys *et al.*, 2013, Servaes *et al.*, 2017), suggesting increased the D_2 receptor signaling (*e.g.*, increased baseline dopamine release) and/or facilitation of D_2 receptor internalization. Accordingly, repeated QNP injection might mimic the abnormal D_2 receptor signaling, resulting in activation of iMSNs.

In iMSNs, the A_{2A} receptor signal contributes to synaptic plasticity (Shen *et al*, 2008). In contrast, the blockade of A_{2A} receptors by istradefylline inhibits iMSNs (Shen *et al*, 2008) and then, facilitates dMSN-mediated signal transduction. A_{2A} receptor signaling in the striatum is involved in the mediation of goal-directed learning and habit formation in naïve mice (Yu *et al.*, 2009; Li *et al.*, 2016), supporting our findings that istradefylline improved the cognitive inflexibility in QNP-treated mice.

Besides cognitive inflexibility, istradefylline improved the SSRI-resistant repetitive chewing behavior, suggesting the therapeutic potential of A_{2A} antagonists for a wide range of OCD symptoms. Future work is needed to determine whether istradefylline and other A_{2A} antagonists show similar therapeutic effects in other OCD-related behaviors

eNeuro Accepted Manuscript

612 and model animals.

613 Recent evidence suggests that A_{2A} receptors and D_2 receptors form heteromers and that
614 a change in the surface expression of this heteromer might be involved in habit
615 formation (He *et al.*, 2016). In A_{2A}-D_2 heteromers, A_{2A} receptor signaling positively
616 modulates D_2 agonist-induced internalization and the resulting intracellular signaling,
617 such as ERK phosphorylation (Borroto-Escuela *et al.*, 2011; Huang *et al.*, 2013). In
618 accordance with this, co-stimulation of A_{2A} receptors and D_2 receptors facilitated
619 repetitive chewing behavior in QNP-sensitized mice. The A_{2A} signaling-mediated
620 internalization of A_{2A}-D_2 heteromers might be involved in OCD pathophysiology and
621 the anti-OCD action of istradefylline; however, further studies are required.

622

623 In conclusion, we characterized distinct treatment responses of OCD-related
624 abnormalities in QNP-treated mice. Chronic high-dose SSRI rescued lOFC
625 hyperactivity, while the therapeutic effect was restricted. An A_{2A} antagonist,
626 istradefylline, normalized synaptic functions in CS iMSNs and improved both the
627 SSRI-responsive and SSRI-resistant OCD-related behaviors in QNP-treated mice.
628 Considering that istradefylline has already been approved as an anti-Parkinsonian agent,
629 the present results support the drug repositioning of istradefylline to be a rapid-acting

eNeuro Accepted Manuscript

630 and effective anti-OCD drug.

631

632 **References**

633 Adams JP, Sweatt JD (2002) Molecular psychology: roles for the ERK MAP kinase
634 cascade in memory. *Annu Rev Pharmacol Toxicol.* **42**: 135-63.

635 Ahmari SE, Spellman T, Douglass NL, Kheirbek MA, Simpson HB, Deisseroth K,
636 Gordon JA, Hen R (2013) Repeated cortico-striatal stimulation generates persistent
637 OCD-like behavior. *Science* **340**: 1234-9.

638 Alonso P, López-Solà C, Real E, Segalàs C, Menchón JM (2015) Animal models of
639 obsessive-compulsive disorder: utility and limitations. *Neuropsychiatr Dis Treat.* **11**:
640 1939-55.

641 Asaoka N, Nishitani N, Kinoshita H, Kawai H, Shibui N, Nagayasu K, Shirakawa H,
642 Nakagawa T, Kaneko S (2017) Chronic antidepressant potentiates spontaneous
643 activity of dorsal raphe serotonergic neurons by decreasing $GABA_B$
644 receptor-mediated inhibition of L-type calcium channels. *Sci Rep.* **7**: 13609.

645 Bannerman DM, Niewoehner B, Lyon L, Romberg C, Schmitt WB, Taylor A, Sanderson
646 DJ, Cottam J, Sprengel R, Seeburg PH, Köhr G, Rawlins JN (2008) NMDA receptor
647 subunit NR2A is required for rapidly acquired spatial working memory but not

eNeuro Accepted Manuscript

incremental spatial reference memory. *J Neurosci.* **28**: 3623-30.

Barraco RA, Martens KA, Parizon M, Normile HJ (1994) Role of adenosine A2a receptors in the nucleus accumbens. *Prog Neuropsychopharmacol Biol Psychiatry.* **18**: 545-53.

Baxter LR Jr, Phelps ME, Mazziotta JC, Guze BH, Schwartz JM, Selin CE (1987) Local cerebral glucose metabolic rates in obsessive-compulsive disorder. A comparison with rates in unipolar depression and in normal controls. *Arch Gen Psychiatry.* **44**: 211-8.

Beucke JC, Sepulcre J, Talukdar T, Linnman C, Zschenderlein K, Endrass T, Kaufmann C, Kathmann N (2013) Abnormally high degree connectivity of the orbitofrontal cortex in obsessive-compulsive disorder. *JAMA Psychiatry.* **70**: 619-29.

Bokor G, Anderson PD (2014) Obsessive-compulsive disorder. *J Pharm Pract.* **27**: 116-30.

Borroto-Escuela DO, Romero-Fernandez W, Tarakanov AO, Ciruela F, Agnati LF, Fuxe K (2011) On the existence of a possible A_{2A}-D_2-β-Arrestin2 complex A_{2A} agonist modulation of D_2 agonist-induced β-arrestin2 recruitment. *J Mol Biol.* **406**: 687-99.

Boulougouris V, Chamberlain SR, Robbins TW (2009) Cross-species models of OCD spectrum disorders. *Psychiatry Res.* **170**: 15-21.

eNeuro Accepted Manuscript

Brami-Cherrier K, Valjent E, Garcia M, Pagès C, Hipskind RA, Caboche J (2002) Dopamine induces a PI3-kinase-independent activation of Akt in striatal neurons: a new route to cAMP response element-binding protein phosphorylation. *J Neurosci*. **22**: 8911-21.

Burguière E, Monteiro P, Feng G, Graybiel AM (2013) Optogenetic stimulation of lateral orbitofronto-striatal pathway suppresses compulsive behaviors. *Science* **340**: 1243-6.

Calabresi P, Picconi B, Tozzi A, Ghiglieri V, Di Filippo M (2014) Direct and indirect pathways of basal ganglia: a critical reappraisal. *Nat Neurosci.* **17**: 1022-30.

Camilla d'Angelo LS, Eagle DM, Grant JE, Fineberg NA, Robbins TW, Chamberlain SR (2014) Animal models of obsessive-compulsive spectrum disorders. *CNS Spectr.* **19**: 28-49.

Chen JF, Moratalla R, Impagnatiello F, Grandy DK, Cuellar B, Rubinstein M, Beilstein MA, Hackett E, Fink JS, Low MJ, Ongini E, Schwarzschild MA (2001) The role of the D_2 dopamine receptor (D_2R) in A_{2A} adenosine receptor ($A_{2A}R$)-mediated behavioral and cellular responses as revealed by A_{2A} and D_2 receptor knockout mice. *Proc Natl Acad Sci U S A.* **98**: 1970-5.

Chuhma N, Mingote S, Kalmbach A, Yetnikoff L, Rayport S (2017). Heterogeneity in

eNeuro Accepted Manuscript

684 Dopamine Neuron Synaptic Actions Across the Striatum and Its Relevance for
685 Schizophrenia. *Biol Psychiatry.* **81**: 43-51.

686 Denys D, van der Wee N, Janssen J, De Geus F, Westenberg HG (2004) Low level of
687 dopaminergic D_2 receptor binding in obsessive-compulsive disorder. *Biol Psychiatry.*
688 **55**: 1041-5.

689 Denys D, de Vries F, Cath D, Figee M, Vulink N, Veltman DJ, van der Doef TF,
690 Boellaard R, Westenberg H, van Balkom A, Lammertsma AA, van Berckel BN
691 (2013). Dopaminergic activity in Tourette syndrome and obsessive-compulsive
692 disorder. Eur *Neuropsychopharmacol.* **23**: 1423-31.

693 Fasano A and Petrovic I (2010). Insights into pathophysiology of punding reveal
694 possible treatment strategies. *Mol Psychiatry.* **15**: 560-73.

695 Gillan CM, Kosinski M, Whelan R, Phelps EA, Daw ND (2016) Characterizing a
696 psychiatric symptom dimension related to deficits in goal-directed control. *Elife* **5**:
697 e11305.

698 Gillan CM, Papmeyer M, Morein-Zamir S, Sahakian BJ, Fineberg NA, Robbins TW, de
699 Wit S (2011) Disruption in the balance between goal-directed behavior and habit
700 learning in obsessive-compulsive disorder. *Am J Psychiatry.* **168**: 718-26.

701 Gourley SL, Taylor JR (2016) Going and stopping: Dichotomies in behavioral control

eNeuro Accepted Manuscript

by the prefrontal cortex. *Nat Neurosci.* **19**: 656-664.

Graybiel AM, Rauch SL (2000) Toward a Neurobiology of Obsessive-Compulsive Disorder. *Neuron* **28**: 343-7.

Gremel CM, Chancey JH, Atwood BK, Luo G, Neve R, Ramakrishnan C, Deisseroth K, Lovinger DM, Costa RM (2016) Endocannabinoid Modulation of Orbitostriatal Circuits Gates Habit Formation. *Neuron* **90**: 1312-1324.

Gremel CM, Costa RM (2013) Orbitofrontal and striatal circuits dynamically encode the shift between goal-directed and habitual actions. *Nat Commun.* **4**: 2264.

He Y, Li Y, Chen M, Pu Z, Zhang F, Chen L, Ruan Y, Pan X, He C, Chen X, Li Z, Chen JF (2016) Habit Formation after Random Interval Training Is Associated with Increased Adenosine A_{2A} Receptor and Dopamine D_2 Receptor Heterodimers in the Striatum. *Front Mol Neurosci.* **9**: 151.

Huang L, Wu DD, Zhang L, Feng LY (2013) Modulation of A_{2a} receptor antagonist on D_2 receptor internalization and ERK phosphorylation. *Acta Pharmacol Sin.* **34**: 1292-300.

Hunnicutt BJ, Jongbloets BC, Birdsong WT, Gertz KJ, Zhong H, Mao T (2016). A comprehensive excitatory input map of the striatum reveals novel functional organization. *Elife.* **5**: e19103.

eNeuro Accepted Manuscript

720 Izawa J, Yamanashi K, Asakura T, Misu Y, Goshima Y (2006). Differential effects of
721 methamphetamine and cocaine on behavior and extracellular levels of dopamine and
722 3,4-dihydroxyphenylalanine in the nucleus accumbens of conscious rats. *Eur J*
723 *Pharmacol.* **549**: 84-90.
724 Kobayashi T, Ikeda K, Ichikawa T, Abe S, Togashi S, Kumanishi T (1995) Molecular
725 cloning of a mouse G-protein-activated K^+ channel (mGIRK1) and distinct
726 distributions of three GIRK (GIRK1, 2 and 3) mRNAs in mouse brain. *Biochem*
727 *Biophys Res Commun.* **208**: 1166-73.
728 Landeros-Weisenberger A, Bloch MH, Kelmendi B, Wegner R, Nudel J, Dombrowski P,
729 Pittenger C, Krystal JH, Goodman WK, Leckman JF, Coric V (2010) Dimensional
730 predictors of response to SRI pharmacotherapy in obsessive-compulsive disorder. *J*
731 *Affect Disord.* **121**: 175-9.
732 Lemos JC, Friend DM, Kaplan AR, Shin JH, Rubinstein M, Kravitz AV, Alvarez VA
733 (2016) Enhanced GABA Transmission Drives Bradykinesia Following Loss of
734 Dopamine D_2 Receptor Signaling. *Neuron* **90**: 824-38.
735 Li Y, He Y, Chen M, Pu Z, Chen L, Li P, Li B, Li H, Huang ZL, Li Z, Chen JF (2016)
736 Optogenetic Activation of Adenosine A_{2A} Receptor Signaling in the Dorsomedial
737 Striatopallidal Neurons Suppresses Goal-Directed Behavior.

eNeuro Accepted Manuscript

738 *Neuropsychopharmacology* **41**: 1003-13.

739 Milad MR, Rauch SL (2012) Obsessive-compulsive disorder: beyond segregated
740 cortico-striatal pathways. *Trends Cogn Sci.* **16**: 43-51.

741 Milesi-Hallé A, McMillan DE, Laurenzana EM, Byrnes-Blake KA, Owens SM (2007).
742 Sex differences in (+)-amphetamine- and (+)-methamphetamine-induced behavioral
743 response in male and female Sprague-Dawley rats. *Pharmacol Biochem Behav*. **86**:
744 140-9.

745 Miyazaki KW, Miyazaki K, Tanaka KF, Yamanaka A, Takahashi A, Tabuchi S, Doya K
746 (2014) Optogenetic activation of dorsal raphe serotonin neurons enhances patience
747 for future rewards. *Curr Biol.* **24**: 2033-40.

748 Moreau JL, Huber G (1999) Central adenosine A_{2A} receptors: an overview. *Brain Res*
749 *Brain Res Rev.* **31**: 65-82.

750 Moy SS, Nadler JJ, Young NB, Perez A, Holloway LP, Barbaro RP, Barbaro JR, Wilson
751 LM, Threadgill DW, Lauder JM, Magnuson TR, Crawley JN (2007) Mouse
752 behavioral tasks relevant to autism: phenotypes of 10 inbred strains. *Behav Brain Res.*
753 **176**: 4-20.

754 Nair AB, Jacob S (2016). A simple practice guide for dose conversion between animals
755 and human. *J Basic Clin Pharm.* **7**: 27-31.

eNeuro Accepted Manuscript

Nielen MM, den Boer JA, Smid HG (2009) Patients with obsessive-compulsive disorder are impaired in associative learning based on external feedback. *Psychol Med.* **39**: 1519-26.

O'Hare JK, Ade KK, Sukharnikova T, Van Hooser SD, Palmeri ML, Yin HH, Calakos N (2016) Pathway-Specific Striatal Substrates for Habitual Behavior. Neuron. **89**: 472-9.

Pallanti S, Hollander E, Goodman WK (2004) A qualitative analysis of nonresponse: management of treatment-refractory obsessive-compulsive disorder. *J Clin Psychiatry.* **65**: 6-10.

Pauls DL, Abramovitch A, Rauch SL, Geller DA (2014) Obsessive-compulsive disorder: an integrative genetic and neurobiological perspective. *Nat Rev Neurosci.* **15**: 410-24.

Plassmann H, O'Doherty J, Shiv B, Rangel A (2008) Marketing actions can modulate neural representations of experienced pleasantness. *Proc Natl Acad Sci U S A.* **105**: 1050-4.

Rauch SL, Shin LM, Dougherty DD, Alpert NM, Fischman AJ, Jenike MA (2002) Predictors of fluvoxamine response in contamination-related obsessive compulsive disorder: a PET symptom provocation study. *Neuropsychopharmacology* **27**: 782-91.

eNeuro Accepted Manuscript

774 Renteria R, Baltz ET, Gremel CM (2018) Chronic alcohol exposure disrupts top-down
775 control over basal ganglia action selection to produce habits. *Nat Commun.* **9**: 211.
776 Saxena S, Brody AL, Maidment KM, Dunkin JJ, Colgan M, Alborzian S, Phelps ME,
777 Baxter LR Jr (1999) Localized orbitofrontal and subcortical metabolic changes and
778 predictors of response to paroxetine treatment in obsessive-compulsive disorder.
779 *Neuropsychopharmacology* **21**: 683-93.
780 Servaes S, Glorie D, Verhaeghe J, Stroobants S, Staelens S (2017) Preclinical molecular
781 imaging of glutamatergic and dopaminergic neuroreceptor kinetics in obsessive
782 compulsive disorder. *Prog Neuropsychopharmacol Biol Psychiatry*. **77**: 90-98.
783 Shan Q, Christie MJ, Balleine BW (2015) Plasticity in striatopallidal projection neurons
784 mediates the acquisition of habitual actions. Eur J Neurosci. 42: 2097-104.
785 Shen W, Flajolet M, Greengard P, Surmeier DJ (2008) Dichotomous dopaminergic
786 control of striatal synaptic plasticity. *Science* **321**: 848-51.
787 Shioda N, Yabuki Y, Wang Y, Uchigashima M, Hikida T, Sasaoka T, Mori H, Watanabe
788 M, Sasahara M, Fukunaga K (2017) Endocytosis following dopamine D_2 receptor
789 activation is critical for neuronal activity and dendritic spine formation via
790 Rabex-5/PDGFRβ signaling in striatopallidal medium spiny neurons. *Mol Psychiatry*
791 **22**: 1205-1222.

eNeuro Accepted Manuscript

792 Smith KS, Virkud A, Deisseroth K, Graybiel AM (2012) Reversible online control of
793 habitual behavior by optogenetic perturbation of medial prefrontal cortex. *Proc Natl*
794 *Acad Sci U S A.* **109**: 18932-7.
795 Starcevic V, Brakoulias V (2008) Symptom subtypes of obsessive-compulsive disorder:
796 are they relevant for treatment? *Aust N Z J Psychiatry.* **42**: 651-61.
797 Stuchlik A, Radostová D, Hatalova H, Vales K, Nekovarova T, Koprivova J, Svoboda J,
798 Horacek J. (2016) Validity of Quinpirole Sensitization Rat Model of OCD: Linking
799 Evidence from Animal and Clinical Studies. *Front Behav Neurosci.* **10**: 209.
800 Szechtman H, Sulis W, Eilam D (1998) Quinpirole induces compulsive checking
801 behavior in rats: a potential animal model of obsessive-compulsive disorder (OCD).
802 *Behav Neurosci.* **112**: 1475-85.
803 Szechtman H, Talangbayan H, Canaran G, Dai H, Eilam D (1994) Dynamics of
804 behavioral sensitization induced by the dopamine agonist quinpirole and a proposed
805 central energy control mechanism. *Psychopharmacology (Berl).* **115**: 95-104.
806 Tateno T, Robinson HP (2006) Rate coding and spike-time variability in cortical
807 neurons with two types of threshold dynamics. *J Neurophysiol.* **95**: 2650-63.
808 Ursu S, Carter CS (2005) Outcome representations, counterfactual comparisons and the
809 human orbitofrontal cortex: implications for neuroimaging studies of

eNeuro Accepted Manuscript

decision-making. *Brain Res Cogn Brain Res.* **23**: 51-60.

Van Ameringen M, Patterson B, Simpson W (2014) DSM-5 obsessive-compulsive and related disorders: clinical implications of new criteria. *Depress Anxiety.* **31**: 487-93.

Voon V, Fernagut PO, Wickens J, Baunez C, Rodriguez M, Pavon N, Juncos JL, Obeso JA, Bezard E (2009). Chronic dopaminergic stimulation in Parkinson's disease: from dyskinesias to impulse control disorders. *Lancet Neurol.* **8**: 1140-9.

Welch JM, Lu J, Rodriguiz RM, Trotta NC, Peca J, Ding JD, Feliciano C, Chen M, Adams JP, Luo J, Dudek SM, Weinberg RJ, Calakos N, Wetsel WC, Feng G (2007) Cortico-striatal synaptic defects and OCD-like behaviours in *Sapap3*-mutant mice. *Nature*. **448**: 894-900.

Yu C, Gupta J, Chen JF, Yin HH (2009) Genetic deletion of A_{2A} adenosine receptors in the striatum selectively impairs habit formation. *J Neurosci.* **29**: 15100-3.

Zike ID, Chohan MO, Kopelman JM, Krasnow EN, Flicker D, Nautiyal KM, Bubser M, Kellendonk C, Jones CK, Stanwood G, Tanaka KF, Moore H, Ahmari SE, Veenstra-VanderWeele J (2017). OCD candidate gene *SLC1A1*/EAAT3 impacts basal ganglia-mediated activity and stereotypic behavior. *Proc Natl Acad Sci U S A.* **114**: 5719-5724.

eNeuro Accepted Manuscript

828 **Figure legends**

829 **Figure 1**

830 Electrophysiological characteristics of lOFC pyramidal neurons and fast-spiking

831 interneurons

832 (**A-C**) Representative firing activity recorded from a pyramidal neuron (**A**; 200 pA

833 injection) and fast-spiking interneuron (**B**; 100 pA injection, **C**; 200 pA injection). (**D**)

834 Current injection-induced firing activity of pyramidal neurons and fast-spiking

835 interneurons. Please note that the data set for pyramidal neurons is same as that in Fig.

836 4B (Saline group). (Pyramidal neurons; $n = 10$ from 3 mice, Fast-spiking interneurons;

837 $n = 5$ from 3 mice.)

838

839 **Figure 2**

840 Representative single-cell PCR from a CS dMSN and iMSN.

841 Representative image of single-cell PCR from CS MSNs. *Pdyn*-positive neurons were

842 considered direct-pathway MSNs (dMSNs; **A**), while *Pdyn*-negative and *Penk*-positive

843 neurons were considered indirect-pathway MSNs (iMSNs; **B**).

844

845 **Figure 3**

846 Repeated injection of QNP elicited multiple OCD-related symptoms.

eNeuro Accepted Manuscript

(**A**) Time course of the elevated plus maze test and open field test. (**B, C**) Time spent in the closed arm (**B**) and the open arm (**C**) in an elevated plus maze test. (**D**) Total travel distance in the open field test. (Saline; n = 5, QNP; n = 5, **B**: Student's *t*-test; $t(8) = 2.178$, $P = 0.0610$, **C**: Student's *t*-test; $t(8) = 0.8863$, $P = 0.4013$, **D**: Student's *t*-test; $t(8) = 4.343$, $P = 0.0025$.) (**E**) Time course of recording of QNP-induced repetitive behavior. (**F,G**) Time spent chewing during the 20-30 min after the 1st-8th QNP injection (**F**) and, before and after the 8th QNP injection (**G**). (**F**: Saline; $n = 6$, QNP; $n = 7$, two-way repeated measures ANOVA; Drug ($F_{(1, 24.32)} = 37.18$, $P < 0.0001$), Injection number ($F_{(2.21, 53.75)} = 22.41$, $P < 0.0001$), Interaction ($F_{(2.21, 53.75)} = 20.95$, $P < 0.0001$), Bonferroni post-test; $P^{*} < 0.05$ and $P^{***} < 0.001$, **G**: $n = 4$, one-way repeated measures ANOVA; $F_{(6, 18)} = 38.61$, $P < 0.0001$, Tukey's multiple comparison test; $P^{**} < 0.01$, $P^{**} < 0.001$ vs. Pre.) (**H**) Time course of recording for QNP-induced repetitive behavior combined with short-term administration of diazepam and citalopram. (**I**) Effects of the short-term administration of an antianxiety agent, diazepam (Dzp; 0.3 mg/kg) and an antidepressant, citalopram (Cit; 10 mg/kg) on repetitive behavior in QNP-treated mice. (QNP+Saline; n = 4, QNP+Dzp; n = 4, QNP+Cit; n = 4, two-way repeated measures ANOVA; Drug ($F(2, 36) = 0.41$, $P = 0.6748$), Injection number ($F(2, 36) = 0.56$, $P = 0.5786$), Interaction ($F(2, 36) = 0.42$, $P = 0.7918$)) (**J,K**) Protocols and percentage of

eNeuro Accepted Manuscript

correct choice during training with daily injection of QNP. (Saline; $n = 4$, QNP; $n = 4$, **K**: two-way repeated measures ANOVA; Drug ($F_{(1, 20.23)} = 0.01$, $P = 0.9224$), Injection number ($F_{(3.37, 68.17)} = 9.04$, $P = 0.0004$), Interaction ($F_{(3.37, 68.17)} = 1.66$, $P = 0.2037$)) **(L)** Protocols of a spatial discrimination task and a reversal learning test. (**M,N**) Percentage of correct choice during overtraining (**M**) and reversal learning (**N**). (Saline; $n = 6$, QNP; $n = 5$, **M**: two-way repeated measures ANOVA; Drug ($F_{(1, 25.63)} = 0.07$, $P = 0.8025$), Session number ($F_{(2.85, 73.04)} = 1.93$, $P = 0.1519$), Interaction ($F_{(2.85, 73.04)} = 1.58$, $P = 0.2201$), **N**: two-way repeated measures ANOVA; Drug ($F_{(1, 36)} = 10.46$, $P = 0.0102$), Session number ($F_{(4, 144)} = 34.86$, $P < 0.0001$), Interaction ($F_{(4, 144)} = 4.29$, $P = 0.0061$), Bonferroni post-test; $P^{**} < 0.01$.)

Figure 4

Hyperactivity of lOFC pyramidal neurons in QNP-treated mice

(**A**) Time course of electrophysiological recordings. (**B,C**) Current injection induced firing activity of lOFC pyramidal neurons in the absence (**B**) and presence (**C**) of AMPA/NMDA antagonists. (**B**: Saline; $n = 10$ from 3 mice, QNP; $n = 10$ from 3 mice, two-way repeated measures ANOVA; Drug ($F_{(1, 36.27)} = 6.15$, $P = 0.0227$), Current ($F_{(1.91, 69.27)} = 324.00$, $P < 0.0001$), Interaction ($F_{(1.91, 69.27)} = 4.07$, $P = 0.0270$), Bonferroni

eNeuro Accepted Manuscript

883 post-test; $P^{*} < 0.05$ and $P^{**} < 0.01$, C: Saline; $n = 11$ from 3 mice, QNP; $n = 10$ from 3
884 mice, two-way repeated measures ANOVA; Drug ($F_{(1, 38.97)} = 0.03$, $P = 0.8743$), Current
885 ($F_{(2.29, 89.24)} = 209.69$, $P < 0.0001$), Interaction ($F_{(2.29, 89.24)} = 0.45$, $P = 0.6660$)) (**D**)
886 Representative traces of spontaneous EPSCs (sEPSCs) and miniature EPSCs (mEPSCs).
887 (**E,F**) sEPSC frequency (**E**) and amplitude (**F**) in lOFC pyramidal neurons. (Saline; n =
888 8 from 3 mice, QNP; n= 15 from 3 mice, **E**: unpaired *t* test with Welch's correction;
889 $t(21) = 2.632$, $P = 0.0160$, **F**: Student's *t*-test; $t(21) = 0.7675$, $P = 0.4513$.) (**G,H**)
890 mEPSC frequency (**G**) and amplitude (**H**) in lOFC pyramidal neurons. (Saline; n = 7
891 from 3 mice, QNP; n= 9 from 3 mice, **G**: Student's *t*-test; $t(14) = 2.740$, $P = 0.0160$, **H**:
892 Student's *t*-test; $t(14) = 1.277$, $P = 0.2223$.)
893
894 **Figure 5**
895 Chronic SSRI treatment rescued cognitive inflexibility in QNP-treated mice but not the
896 abnormal repetitive behavior.
897 (**A**) Time course of recording for QNP-induced repetitive behavior combined with
898 chronic SSRI administration. (**B**) Time spent chewing during the 20-30 min after the 8th
899 QNP injection. (Water+Saline; n = 7, Cit+Saline; n= 6, Water+QNP; n = 7, Cit+QNP;
900 n= 6, two-way ANOVA; p.o. administration ($F_{(1, 22)} = 0.56$, $P = 0.4616$), i.p. injection

eNeuro Accepted Manuscript

($F_{(1, 22)}$ = 727.10, P < 0.0001), Interaction ($F_{(1, 22)}$ = 0.11, P = 0.7440), Bonferroni post-test; not significant (n.s.)) (**C**) Time course of a spatial discrimination task and a reversal learning test combined with chronic SSRI administration. (**D,E**) Percentage of correct choices during overtraining (**D**) and reversal learning (**E**). (Water+QNP; n = 5, Cit+QNP; n= 5, **D**: two-way repeated measures ANOVA; Drug ($F_{(1, 26.9)}$ = 2.47, P = 0.1547), Session number ($F_{(3.36, 90.38)}$ = 1.27, P = 0.3040), Interaction ($F_{(3.36, 90.38)}$ = 0.62, P = 0.6233), **E**: two-way repeated measures ANOVA; Drug ($F_{(1, 32)}$ = 9.71, P = 0.0143), Session number ($F_{(4, 128)}$ = 48.66, P < 0.0001), Interaction ($F_{(4, 128)}$ = 1.63, P = 0.1920), Bonferroni post-test; P^{*} < 0.05.)

Figure 6

Chronic SSRI treatment rescued lOFC hyperactivity in QNP-treated mice

(**A**) Time course of electrophysiological recordings combined with chronic SSRI administration. (**B,C**) Current injection induced firing activity of lOFC pyramidal neurons in the absence (**B**) and presence (**C**) of $GABA_A$ antagonists. (**B**: Water+QNP; n = 8 from 3 mice, Cit+QNP; n = 12 from 3 mice, two-way repeated measures ANOVA; Drug ($F_{(1, 27.96)}$ = 6.96, P = 0.0167), Current ($F_{(1.55, 43.34)}$ = 309.92, P < 0.0001), Interaction ($F_{(1.55, 43.34)}$ = 4.04, P = 0.0297), Bonferroni post-test; P^{*} < 0.05 and P^{**} <

eNeuro Accepted Manuscript

0.01, **C**: Water+QNP; n = 11 from 3 mice, Cit+QNP; n = 11 from 3 mice, two-way repeated measures ANOVA; Drug ($F_{(1, 40.58)}$ = 0.00, P = 0.9673), Current ($F_{(2.03, 82.38)}$ = 250.93, P < 0.0001), Interaction ($F_{(2.03, 82.38)}$ = 0.12, P = 0.8889)) (**D**) Representative traces of sIPSCs and mIPSCs. (**E,F**) sIPSC frequency (**E**) and amplitude (**F**) in lOFC pyramidal neurons. (Water+Saline; n = 14 from 3 mice, Water+QNP; n = 17 from 3 mice, Cit+QNP; n = 15 from 3 mice, **E**: one-way ANOVA; $F_{(2, 43)}$ = 3.758, P = 0.0313, Tukey's multiple comparison test; P^* < 0.05, **F**: one-way ANOVA; $F_{(2, 43)}$ = 0.1188, P = 0.8883.) (**G,H**) mIPSC frequency (**G**) and amplitude (**H**) in lOFC pyramidal neurons. (**G**: Water+Saline; n = 12 from 3 mice, Water+QNP; n = 13 from 3 mice, Cit+QNP; n = 11 from 3 mice, one-way ANOVA; $F_{(2, 33)}$ = 0.2934, P = 0.7476, **H**: Water+Saline; n = 12 from 3 mice, Water+QNP; n = 11 from 3 mice, Cit+QNP; n = 10 from 3 mice, one-way ANOVA; $F_{(2, 30)}$ = 0.1310, P = 0.8777.)

Figure 7

D_2-ERK signaling in the CS was required for repetitive behavior in QNP-treated mice

(**A,B**) Representative images from AAV-hSyn-Venus mediated labeling of lOFC neurons. Green fluorescence was observed at both the AAV injection site (**A**; lOFC) and the striatal projection site (**B**; CS). Scale bar = 100 μm (**B**; center) and 20 μm (**B**; right).

eNeuro Accepted Manuscript

(**C**) Time course of stereotaxic surgery and recording of QNP-induced repetitive behavior combined with intra-CS local drug injection. (**D,E**) Effect of intra-CS injection of racroprode (Rac; 1 μg/side) or PD98059 (1 μg/side) on repetitive chewing behavior in QNP-treated mice. (**D**: n = 5, paired *t* test; $t(5) = 15.31$, $P < 0.0001$, **E**: n = 5, paired *t* test; $t(5) = 3.643$, $P = 0.0070$.) (**F**) Time course of recording of low-dose QNP-induced chewing behavior. (**G**) Time spent chewing during the 20-30 min after the 8^{th}-10^{th} QNP injection (1.0, 0.5, 0.3 mg/kg respectively). n = 5. (**H**) Time course of stereotaxic surgery and recording of intra-CS local injection-induced repetitive behavior combined with subthreshold dose of QNP injection. (**I**) Time spent chewing during the 20-30 min after intra-CS injection of CGS 21680A (CGS; 0.3 ng/side) and subthreshold dose of QNP injection (0.3 mg/kg). n = 3, paired *t* test; $t(2) = 4.395$, $P = 0.0481$.

Figure 8

Istradefylline rescued both the behavioral and cognitive symptoms in QNP-treated mice. (**A**) Time course of recording of QNP-induced repetitive behavior combined with the short-term administration of istradefylline (Ist). (**B**) Time spent chewing during 20-30 min after QNP and Ist injections. (QNP+Veh; $n = 5$, QNP+Ist; $n = 4$, two-way repeated measures ANOVA; Drug ($F_{(1, 8.05)} = 27.48$, $P = 0.0012$), Injection number ($F_{(1.15, 9.26)} =$

eNeuro Accepted Manuscript

17.45, P = 0.0025), Interaction ($F_{(1.15, 9.26)}$ = 17.78, P = 0.0024), Bonferroni post-test; P^{**} < 0.01, P^{***} < 0.001.) (**C**) Time course of a spatial discrimination task and a reversal learning test combined with the short-term administration of Ist. (**D,E**) Percentage of correct choices during over training (**D**) and reversal learning (**E**). (QNP+Veh; n = 5, QNP+Ist; n = 6, **D**: two-way repeated measures ANOVA; Drug ($F_{(1, 25.01)}$ = 0.72, P = 0.4175), Session number ($F_{(2.78, 69.53)}$ = 0.78, P = 0.5068), Interaction ($F_{(2.78, 69.53)}$ = 1.04, P = 0.3878)), **E**: two-way repeated measures ANOVA; Drug ($F_{(1, 36)}$ = 7.29, P = 0.0244), Session number ($F_{(4, 144)}$ = 68.34, P < 0.0001), Interaction ($F_{(4, 144)}$ = 1.58, P = 0.2010))

Figure 9

Altered synaptic functions in the CS iMSNs from QNP-treated mice was rescued by an A_{2A} antagonist

(**A**) Time course of electrophysiological recordings from CS MSNs. (**B**) Baseline NMDA/AMPA ratios recorded from CS dMSNs. (Control condition: Saline; n = 6 from 5 mice, QNP; n= 14 from 5 mice, Student's t-test; t(18) = 0.09770, P = 0.9233, PD98059: Saline; n = 12 from 4 mice, QNP; n= 11 from 4 mice, Unpaired t-test with Welch's correction; t(12) = 0.7569, P = 0.4637, Ist (istradefylline): Saline; n = 4 from 3 mice, QNP; n= 6 from 3 mice, Student's t-test; t(8) = 0.6724, P = 0.5203.) (**C**) Bath

eNeuro Accepted Manuscript

application of QNP-induced changes in the NMDA/AMPA ratio recorded from CS dMSNs. (Control condition: Saline; n = 6 from 5 mice, $t(5) = 1.587$, $P = 0.1735$, QNP; n = 14 from 5 mice, $t(13) = 0.3219$, $P = 0.7526$, PD98059: Saline; n = 12 from 4 mice, $t(11) = 0.2176$, $P = 0.8317$, QNP; n = 11 from 4 mice, $t(10) = 0.03232$, $P = 0.9748$, Ist: Saline; n = 4 from 3 mice, $t(3) = 0.1016$, $P = 0.9255$, QNP; n = 6 from 3 mice, $t(5) = 0.5138$, $P = 0.6293$. One sample t-test compared with 100.) (**D**) Baseline NMDA/AMPA ratios recorded from CS iMSNs. (Control condition: Saline; n = 7 from 3 mice, QNP; n= 5 from 4 mice, Student's t-test; $t(10) = 5.067$, $P = 0.0005$, PD98059: Saline; n = 6 from 4 mice, QNP; n= 5 from 3 mice, Unpaired t-test with Welch's correction; $t(6) = 2.277$, $P = 0.0630$, Ist: Saline; n = 4 from 3 mice, QNP; n= 6 from 3 mice, Student's t-test; $t(8) = 0.3501$, $P = 0.7353$.) (**E**) Bath application of QNP-induced changes in the NMDA/AMPA ratio recorded from CS iMSNs. (Control condition: Saline; n = 7 from 3 mice, $t(6) = 0.1710$, $P = 0.8699$, QNP; n = 5 from 4 mice, $t(4) = 3.019$, $P = 0.0392$, PD98059: Saline; n = 6 from 4 mice, $t(5) = 0.6388$, $P = 0.5510$, QNP; n = 5 from 3 mice, $t(4) = 0.6333$, $P = 0.5610$, Ist: Saline; n = 4 from 3 mice, $t(3) = 1.547$, $P = 0.2195$, QNP; n = 6 from 3 mice, $t(5) = 1.684$, $P = 0.1529$. One sample t-test compared with 100.)

eNeuro Accepted Manuscript

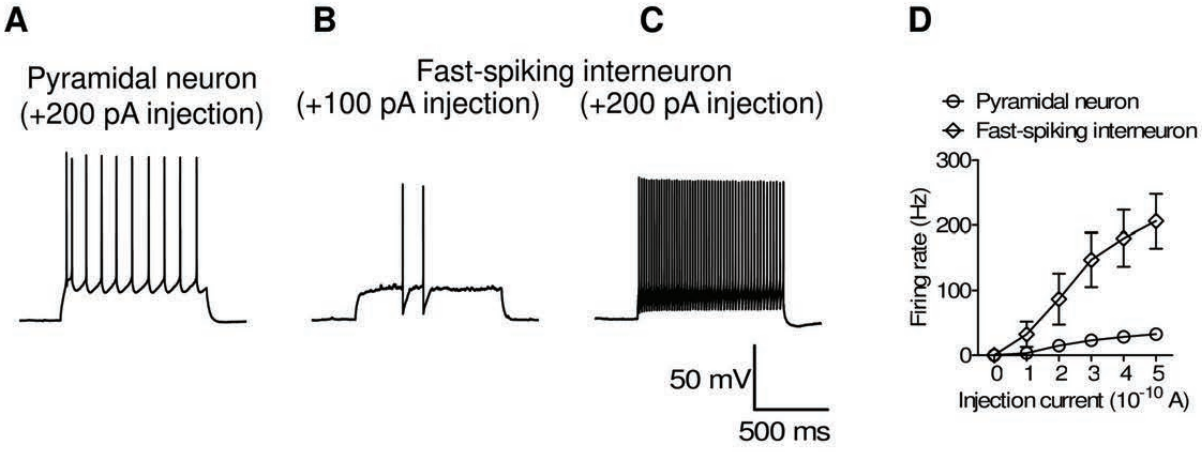

eNeuro Accepted Manuscript

A *Pdyn*-positive neuron (dMSN)

Pdyn (105 bp)
Penk (74 bp)
Eno2 (144 bp)

B *Penk*-positive neuron (iMSN)

Pdyn (105 bp)
Penk (74 bp)
Eno2 (144 bp)

eNeuro Accepted Manuscript

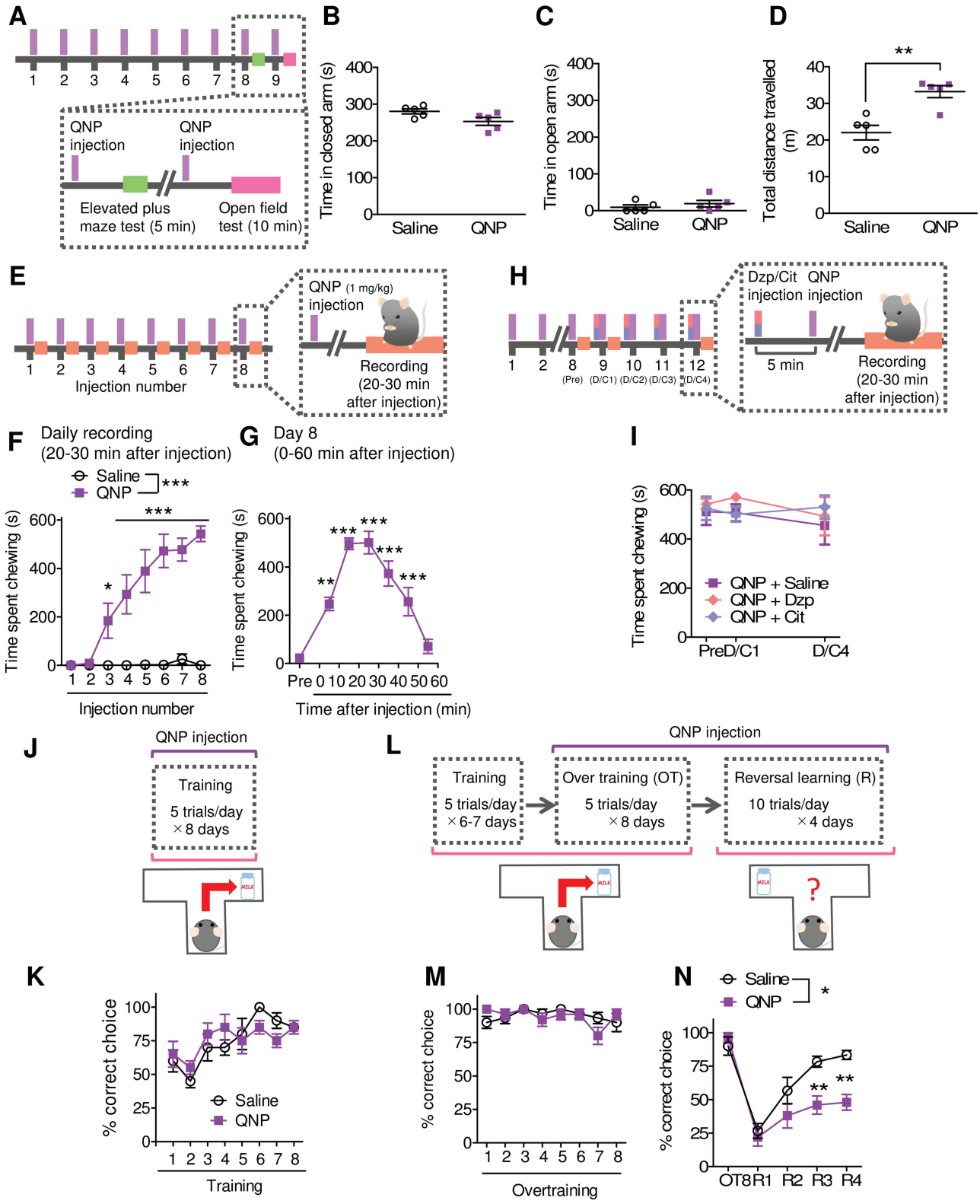

eNeuro Accepted Manuscript

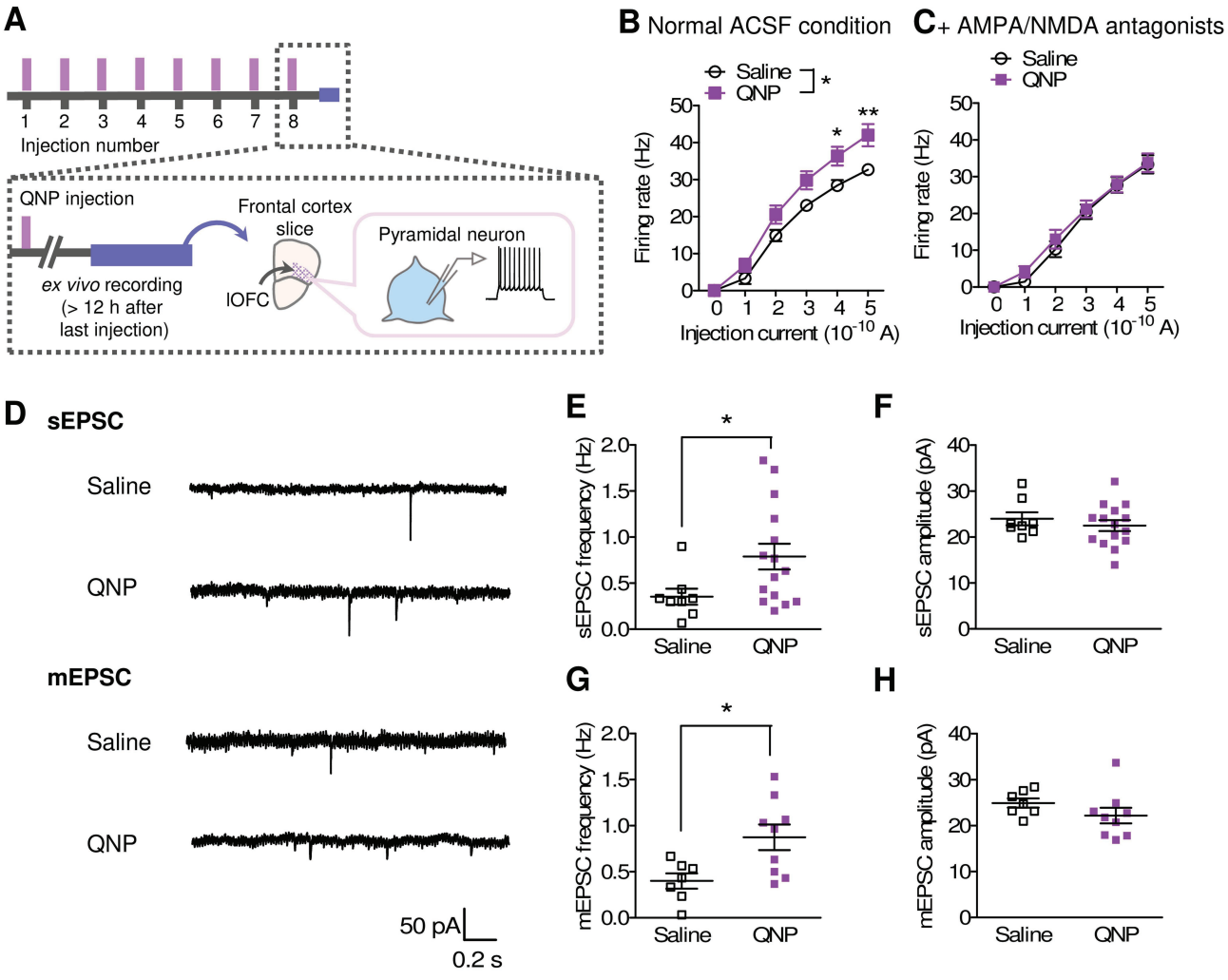

eNeuro Accepted Manuscript

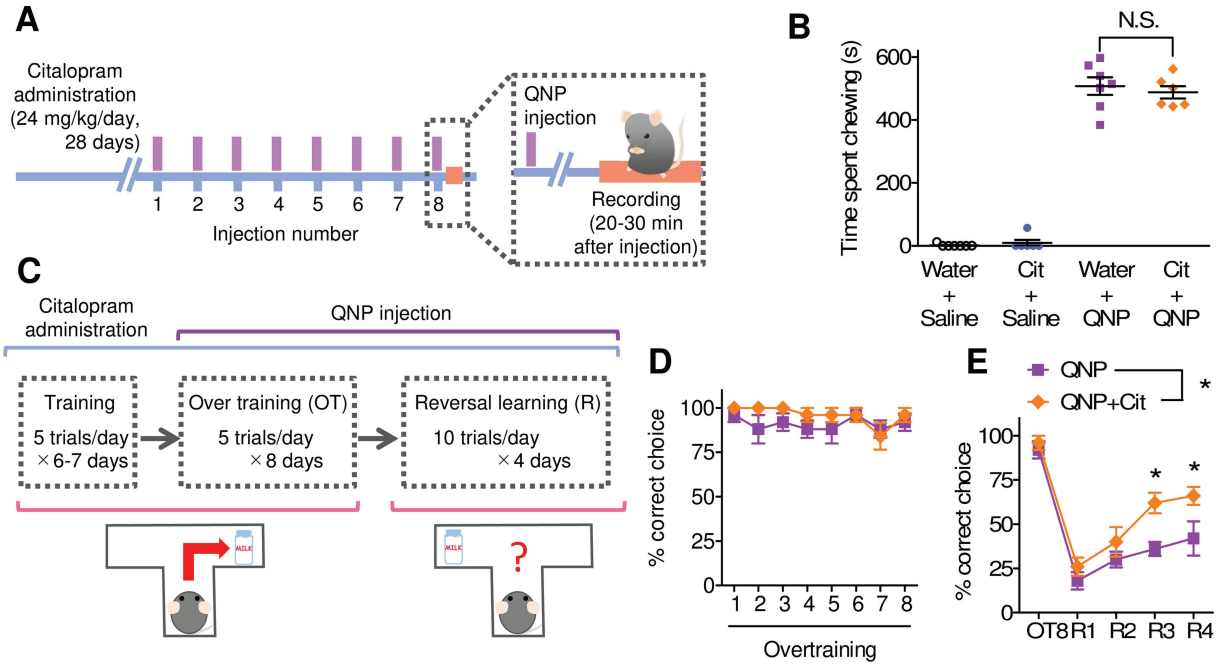

eNeuro Accepted Manuscript

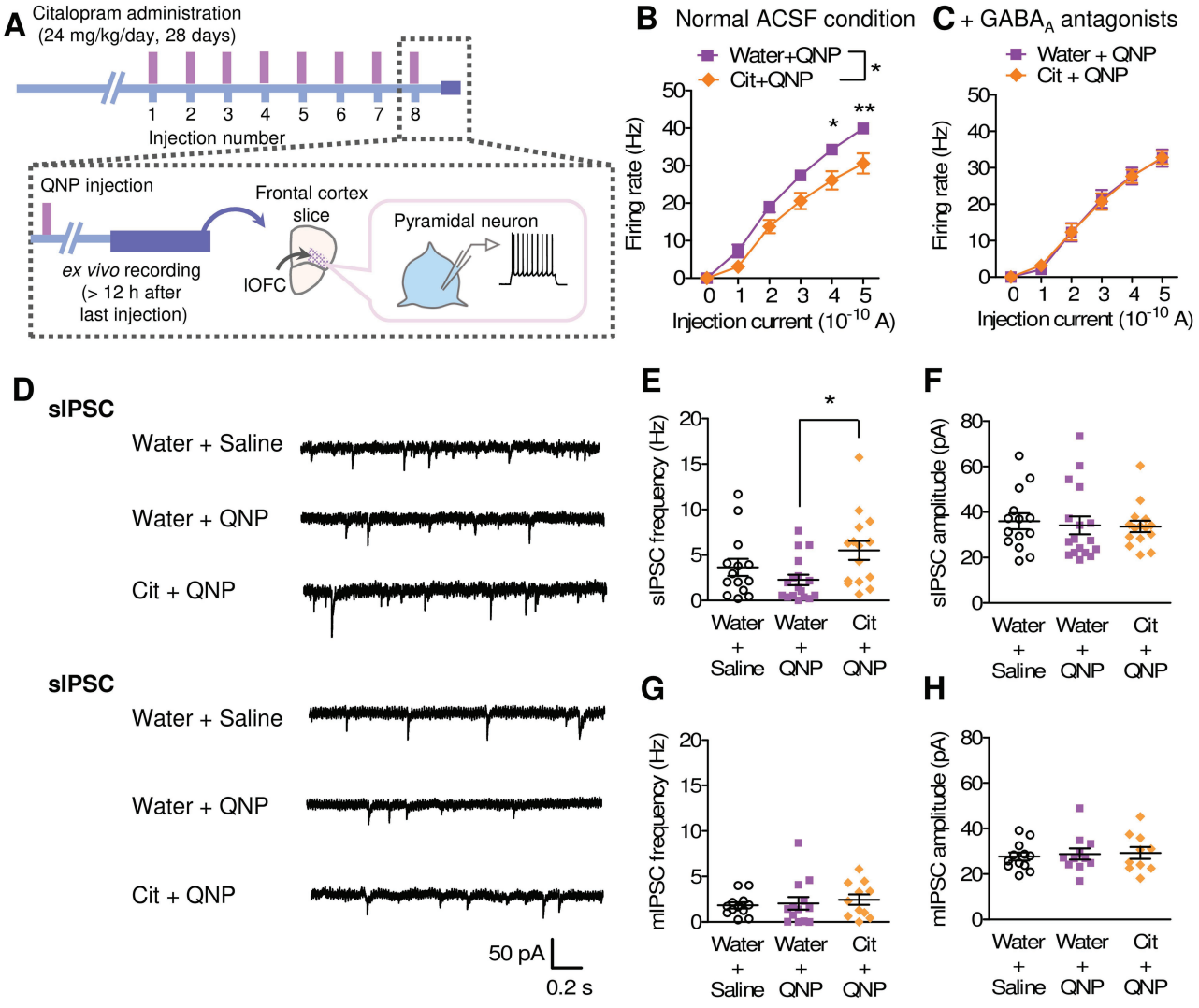

eNeuro Accepted Manuscript

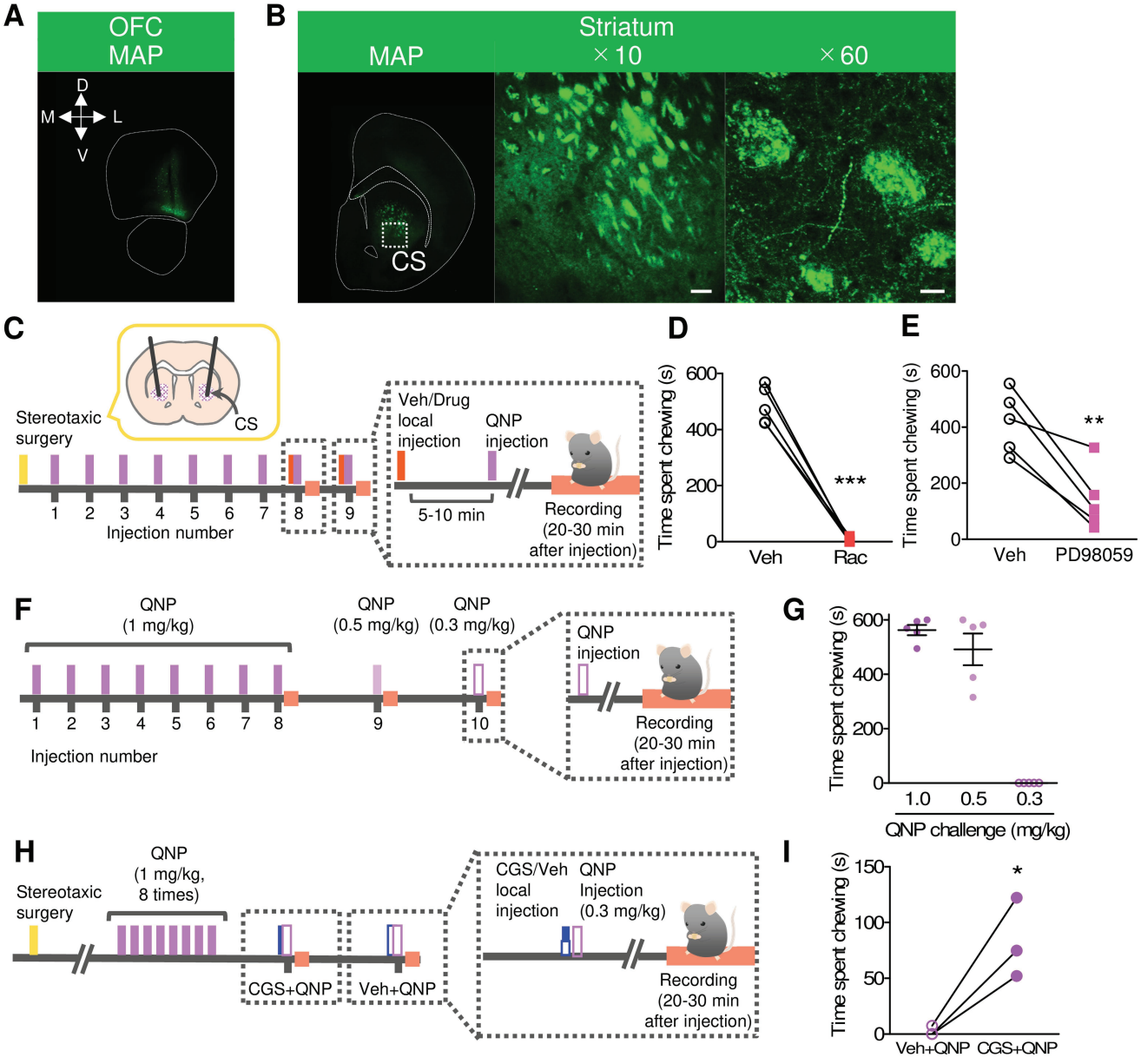

eNeuro Accepted Manuscript

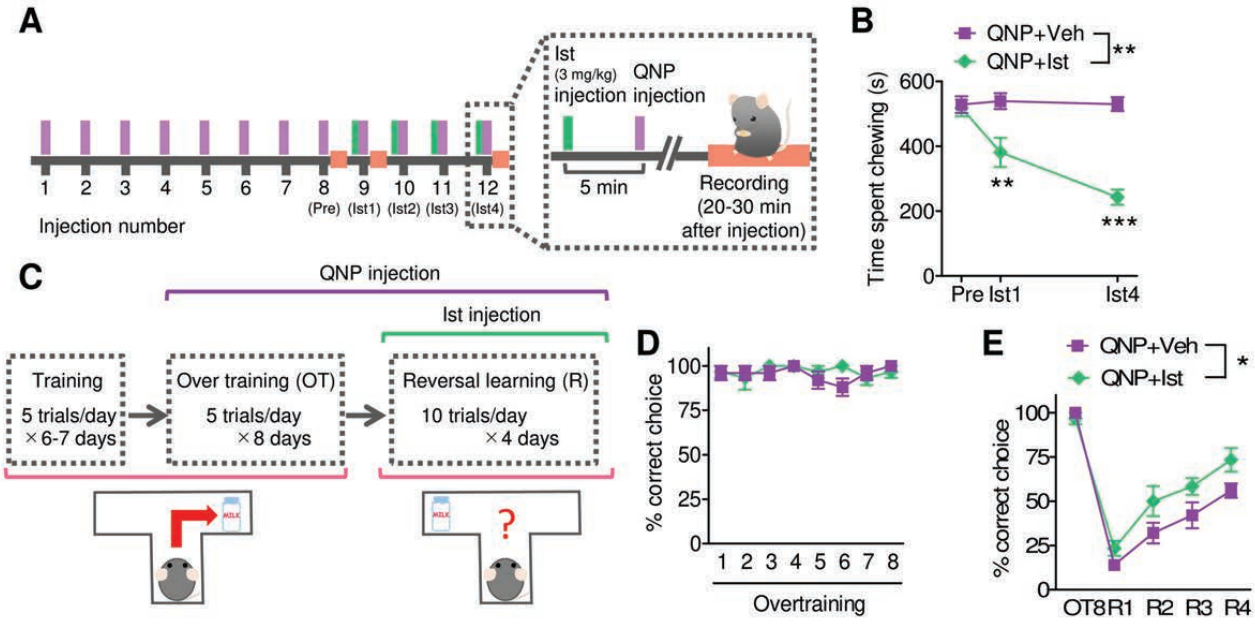

eNeuro Accepted Manuscript